AD_____

AWARD NUMBER: DAMD17-02-1-0570

TITLE: Breast Cancer Detection using Optical Vascular Function

PRINCIPAL INVESTIGATOR: Gregory W. Faris, Ph.D.

CONTRACTING ORGANIZATION: SRI International
Menlo Park, California 94025-3493

REPORT DATE: June 2005

TYPE OF REPORT: Final

PREPARED FOR: U.S. Army Medical Research and Materiel Command
Fort Detrick, Maryland 21702-5012

REPORT DOCUMENTATION PAGE

Form Approved
OMB No. 0704-0188

1. REPORT DATE *(DD-MM-YYYY)*	**2. REPORT TYPE**	**3. DATES COVERED** *(From - To)*
01-06-2005	Final	13 May 2002 – 12 May 2005

4. TITLE AND SUBTITLE

Breast Cancer Detection using Optical Vascular Function

5a. CONTRACT NUMBER

5b. GRANT NUMBER
DAMD17-02-1-0570

5c. PROGRAM ELEMENT NUMBER

6. AUTHOR(S)

Gregory W. Faris, Ph.D.

E-Mail: gregory.faris@sri.com

5d. PROJECT NUMBER

5e. TASK NUMBER

5f. WORK UNIT NUMBER

7. PERFORMING ORGANIZATION NAME(S) AND ADDRESS(ES)

SRI International
Menlo Park, California 94025-3493

8. PERFORMING ORGANIZATION REPORT NUMBER

9. SPONSORING / MONITORING AGENCY NAME(S) AND ADDRESS(ES)
U.S. Army Medical Research and Materiel Command
Fort Detrick, Maryland 21702-5012

10. SPONSOR/MONITOR'S ACRONYM(S)

11. SPONSOR/MONITOR'S REPORT NUMBER(S)

12. DISTRIBUTION / AVAILABILITY STATEMENT
Approved for Public Release; Distribution Unlimited

13. SUPPLEMENTARY NOTES

14. ABSTRACT
We are investigating a new approach to detection of breast cancer using optical vascular function imaging. Research on cancer therapy has revealed unusual properties of tumor vasculature produced through angiogenesis that have high promise for breast cancer detection. We are using this unusual behavior as a contrast mechanism by performing optical imaging during administration of different levels of oxygen and carbon dioxide. We have constructed imaging systems using immersion in a tissue phantom, improved the sensitivity and speed of the imaging systems and used mass flow controllers to regulate inhalation gas compositions, imaged 5 different cancer models, and compared dynamic and static measurements. Our results support our hypothesis that the additional contrast from imaging vascular function is superior to static (conventional) optical imaging. The results of this IDEA project have been the basis of additional funding for clinical testing. We believe that this approach can form the basis for a cancer imaging modality combining high sensitivity and specificity. New, sensitive, specific, and low cost imaging technologies are very important for detection and treatment of breast cancer, and should lead to reduced morbidity and mortality from this disease.

15. SUBJECT TERMS
breast cancer, cancer detection, optical imaging, angiogenesis, functional imaging, animal model, cancer diagnosis

16. SECURITY CLASSIFICATION OF:			**17. LIMITATION OF ABSTRACT**	**18. NUMBER OF PAGES**	**19a. NAME OF RESPONSIBLE PERSON**
a. REPORT	**b. ABSTRACT**	**c. THIS PAGE**			USAMRMC
U	U	U	UU	52	**19b. TELEPHONE NUMBER** *(include area code)*

TABLE OF CONTENTS

INTRODUCTION

We are investigating a new approach to detection of breast cancer using optical vascular function imaging. Research on cancer therapy has revealed unusual properties of tumor vasculature produced through angiogenesis that have high promise for breast cancer detection. We are using this unusual behavior as a contrast mechanism by performing optical imaging during administration of different levels of oxygen and carbon dioxide. We have constructed imaging systems using immersion in a tissue phantom, improved the sensitivity and speed of the imaging systems, used mass flow controllers to regulate inhalation gas compositions, imaged 5 different cancer models, and compared dynamic and static measurements. Our results support our hypothesis that the additional contrast from imaging vascular function is superior to static (conventional) optical imaging. The results of this IDEA project have been the basis of new funding for clinical testing. We believe that this approach can form the basis for a cancer imaging modality combining high sensitivity and specificity. New, sensitive, specific, and low cost imaging technologies are very important for detection and treatment of breast cancer, and should lead to reduced morbidity and mortality from this disease.

BODY

The following sections will briefly summarize the accomplishments on each of the project tasks.

TASK 1. MODIFY AND CONSTRUCT IMAGING SYSTEMS

Two optical systems were used in our studies. These include a frequency domain system for quantification of scattering and absorption, and a CW system for monitoring rapid changes at different wavelengths. Work performed on these systems is summarized below.

The frequency domain apparatus developed in our laboratory measures the optical delay of light through a medium in order to quantitatively determine absorption and scattering properties on human or animal tissue. By measuring the phase shift and amplitude decay of the modulated light, one can extract the scattering and absorption coefficients of the sample. The frequency domain apparatus used in our lab to measure tissue optical properties is sketched in Figure 1. Briefly, an oscillator modulates a laser diode at a radio frequency (RF) of 100 MHz. This modulated light is carried to the sample through an optical fiber, and the resulting scattered light is collected by a different optical fiber, which guides the signal to the detector. This signal is amplified and mixed with a part of the original source in order to extract the amplitude and RF phase of the modulated light. By measuring the changes in the DC and RF amplitudes and the RF phase of the detected signal as a function of source-detector separation, we can determine the absorption and scattering coefficients of the measured tissue region.[1] This frequency-domain system has a precision of better than 1% for measurements on homogeneous tissue phantoms.[2] We have made a number of improvements to this measurement system, which will be discussed in the next section.

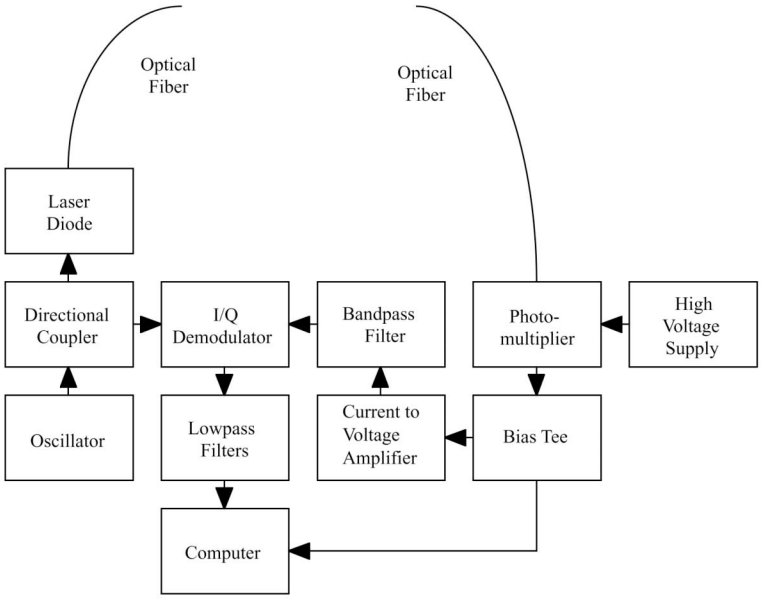

Figure 1. Schematic diagram of the frequency-domain imaging system.

We have constructed a continuous wave immersion imaging system to examine dynamic physiological behavior of rodents. A schematic of the instrument used for immersion imaging is shown below in Figure 2. The imaging system is composed of a light source, an immersion box, and a camera. The light source is made up of arrays of bright light emitting diodes (LED) that emit radiation with peak intensities at three wavelengths: 570 nm, 780 nm, or 840 nm (Epitex). This diffuse, CW light source is directed at the sample immersion box, which contains the animal under study immersed[3] in a heated (37 - 38° C), matching medium (tissue phantom) composed of water, ink, sugar, and submicrometer polymer spheres (Ropaque, Rohm and Haas Company), which approximates the scattering and absorptive properties of the mouse tissue. The front of the immersion box is imaged onto the camera. Images at each individual wavelength are then collected, digitized, and sent to the computer for analysis.

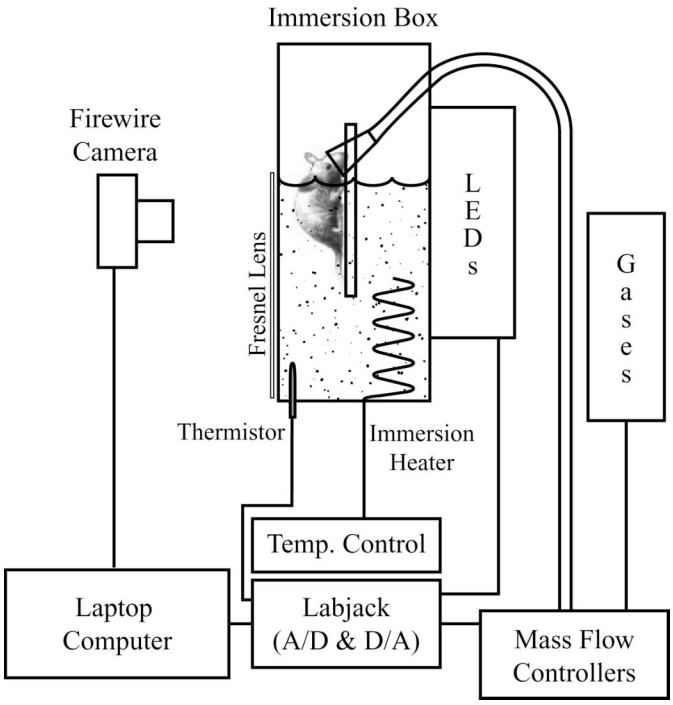

Figure 2. Schematic diagram of the CW immersion imaging system.

The 780 nm and 840 nm wavelengths lie on either side of the isosbestic point for hemoglobin and are intended to provide information on hemoglobin content and hemoglobin oxygenation.[4] The 570 nm wavelength is very strongly attenuated by the hemoglobin in the animal tissues and is much less attenuated in the tissue phantom. This wavelength is intended to provide a images showing the position and outline of the animal while immersed.

TASK 2. IMPROVE IMAGING SYSTEMS

We have made substantial improvements to both the frequency domain and the CW imaging systems. For the frequency domain system, we have rebuilt the detection electronics. The detector is a new, multi-alkali, miniaturized photomultiplier tube (PMT) from Hamamatsu. This tube is more sensitive to the NIR wavelengths used in our experiments. It is also smaller in size, and has a lower electron transit time spread. The output from the PMT, a time-varying current, is directly converted and amplified to a voltage via a wide-bandwidth transimpedance amplifier (Philips). This new detection scheme eliminates two amplifier stages, filters, and

attenuators present in the previous apparatus, and increases the signal-to-noise (S/N) ratio of the detected signals.

Most of the improvements in the CW system have been aimed at complete automation of the experimental apparatus. We have added mass flow controllers (MFC) to the gas lines, which control the exact flow of the individual gas components (air, O_2, and CO_2) to the mouse nose cone. These MFCs are controlled by the computer through a Labview program, which also controls the LEDs and the image acquisition. With the current setup, we can deliver and monitor the gas concentrations delivered to the mouse, monitor the temperature of the immersion bath, and control the LED and camera parameters throughout the duration of the experiment. By carefully controlling and monitoring the experimental variables in our system, we have greatly reduced noise associated with the physiological response of the mouse to its environment. Such improvements have been essential for eliminating external sources of error to our measurements. We have also upgraded the NIR light source to increase the amount of light incident upon the camera. To this end, we have added 3 times the number of LEDs at 780 and 840 nm. We have also added a Fresnel lens onto the front of the immersion box to more effectively couple the scattered light transmitted from the light box onto the CCD camera. This has allowed us to increase the acquisition frame rate and more carefully probe the physiological dynamics of the tissue vasculature.

To improve the sensitivity and speed of the animal imaging experiments we have replaced the Point Grey Instruments Research Dragonfly camera with a QImaging Retiga camera. Between the increased area of the CCD and the higher near infrared quantum efficiency, this change has led to an increased sensitivity by a factor of about 8. The Labview program that controls the experiment was reprogrammed to use the new camera.

TASK 3. PREPARE AND MAINTAIN ANIMAL MODELS

The overall goal of this research is to improve the detection of breast cancer through a non-invasive vascular function imaging system using animal cancer models. *In vivo* xenograft models are useful for these studies because they allow monitoring development (the progressive vascular invasion by tumor cells), including neoplastic contrast on range stage (based on tumor size). These xenograft models also allow us to examine a wide variety of tumors and their unique growing characteristics in order to determine the strengths and weaknesses of the current non-invasive imaging technique. As a model for breast cancer detection, the mice with tumor xenografts are partially immersed in liquid tissue phantoms (media) that simulate the optical properties of breast tissue. Although this approach does not completely include the properties of tissue heterogeneity in the breast, the use of xenograft models are the most practical methods for studying contrast over a range and verity of tumors. In the course of study we also included other non-human breast cancer cells, to help improve technique detection and validation of the imaging system and protocols.

In this work we used two human breast cancer models, an estrogen-dependent cell line (MCF-7) and estrogen-independent cell line (MDA-MB-231) and three other cell lines (mouse embryonic fibrosarcoma, U87 brain cancer, and DLD-1 colon cancer). Our imaging technique examines the vasculature of the tumor through its response to inhalation of carbon dioxide and oxygen. The additional cell lines, particularly the mouse embryonic fibrosarcoma and brain cancer cell lines, have a larger amount of vasculature than the two breast cell lines. In patients, we can expect considerable variability in the amount of tumor vasculature. Thus, including the additional cell lines provides a better indication of the range of response for breast cancer detection in patients.

We had originally proposed to use two animal models for these studies: a human cancer cell line in mice and a chemically induced tumor in rats. Because of the significance of investigating a broad range of tumor vasculature, we have discussed with the Grants Manager for this project substituting the four additional cell line models for the one chemically-induced tumor model. The Grants Manager allowed that this was a small enough change that a formal change to the Statement of Work was not required.

TASK 4. PERFORM ANIMAL IMAGING

Imaging experiments were conducted on animals with tumor volume of 300-1000 mm^3. For each experiment 2-4 animals were used. Prior to imaging, the animals were anesthetized with 40 mg/kg pentobarbital. The mice are then secured to a 3-mm Plexiglas platform with clear surgical tape. The tape used is an improvement over the earlier technique, which employed black nylon tape as an adhesive. The black tape produced regions of contrast following subtraction of a background image, described below. Because we are using a differential measurement to examine changes in tissue optical properties, any movement of the animal generates artifacts in the subtracted measurements. Therefore, anesthesia is given in further doses of 20 mg/kg as needed to reduce stress associated with immersion and to keep the animal immobilized. Using the new computer-controlled apparatus, custom gas mixtures were administered to the immersed mouse via a nose cone at a flow rate of approximately 4.2 l/min. Such a high flow rate was chosen to eliminate rebreathing artifacts. Typically, we cycled between pure air, pure O_2, and carbogen (95% O_2, 5% CO_2). In order to test the different effects of hyperoxia (elevated O_2) versus those of hypercapnia (elevated CO_2), we also have experimented with varying the levels of CO_2 in the presence of O_2 and air, respectively. The optical path length of the immersion box is adjusted to match the thickness of the mouse (~2-2.5 cm). With this thickness, the exposure time of the camera allows us to measure both 780 nm and 840 nm wavelengths at approximately one frame per second. At the end of the experiment

the animals were sacrificed with an overdose of anesthetic agent followed by cervical dislocation.

A background image of individual mice was recorded for each wavelength at the beginning of each experiment. Following background collection, the mouse was imaged during and after the administration of the different gas protocols. From each of these images the background image was subtracted to produce a differential image of the response of the optical properties of the mouse to the different gases. Figure 3, below, demonstrates the enhancement of the imaging contrast with this differential method. The first panel shows one of these static images recorded during the administration of oxygen gas. The outlines of both the mouse and the tumor, determined by recording an image of the animal without the immersion medium, have been placed on top of the image as a guide to the eye. The mouse's head is out of the liquid immersion medium and is at the top of the field of view in the figure. The second panel shows the same image after subtraction of the background. Although the actual boundaries of the mouse and tumor are obscured by the scattering of the immersion medium, it is clear from the difference image in Figure 3b that there are distinct regions of contrast between the tumor and the surrounding tissues of the mouse. While there is a region of enhanced contrast in the first panel due to the static optical properties of the tumor, it is also obvious that the contrast in this region is much greater in the differential image.

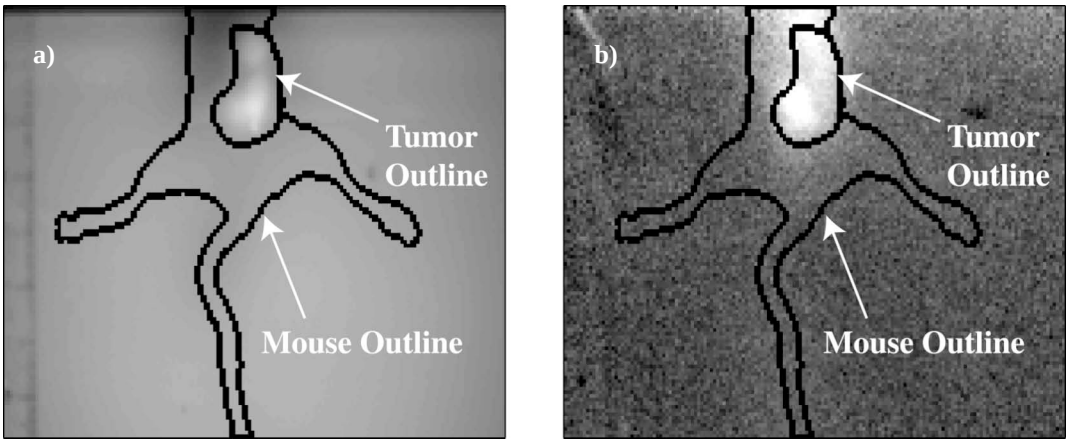

Figure 3. Images of mouse at 840 nm at 100 s after administration of carbogen gas; a) static image; b) image from 3a with background subtracted.

Principal Component Analysis

The imaging experiments described above generated large sets of data. Typically, images with 10^5 pixels at two wavelengths are recorded every 2–10 seconds over the cycling period of carbogen administration (approximately 10 to 20 minutes). Based on these experimental results, we expect to see < 7% change in image intensity following carbogen administration. Because extracting such small signal changes from large data sets poses a formidable challenge, researchers have developed techniques that generate smaller sets of orthogonal images to describe the generated data.[5,6] In practice, these methods have been shown to accurately describe data sets of 10,000 images with only ~100 eigenimages.

In the most basic adaptation of these methods, known as principal component analysis (PCA), the set of recorded images is represented by:

$$f = f(t, \mathbf{x}) \tag{1}$$

where $\boldsymbol{x}$ describes the spatial pixel grayscale values of the image, and t is the time at which the image data was collected. Researchers have shown that these images, $f(t,\mathbf{x})$, can be decomposed into the set of orthogonal functions $a_n(t)$ and $\varphi_n(\mathbf{x})$ by:

$$f(t, \mathbf{x}) = \sum_n \mu_n a_n(t) \varphi_n(\mathbf{x}). \tag{2}$$

A series of T time images containing P pixels can be described by the matrix:

$$\mathbf{M} = \begin{bmatrix} f(1,1) & f(1,2) & \dots & f(1,P) \\ f(2,1) & f(2,2) & \dots & f(2,P) \\ \vdots & & & \vdots \\ f(T,1) & \dots & \dots & f(T,P) \end{bmatrix} \tag{3}$$

This matrix can then be decomposed into the different $a_n(t)$ and $\varphi_n(\mathbf{x})$ components through the general technique of singular value decomposition:

$$\mathbf{A}_n = \begin{bmatrix} a_n(1) \\ \vdots \\ a_n(T) \end{bmatrix}, \ \mathbf{V}_n = \begin{bmatrix} \varphi_n(1) \\ \vdots \\ \varphi_n(P) \end{bmatrix}, \text{ and } \mathbf{U} = \begin{bmatrix} \mu_1 & & 0 \\ & \ddots & \\ 0 & & \mu_T \end{bmatrix} \tag{4}$$

and

$$\mathbf{M}=\mathbf{AUV}^{\dagger} \tag{5}$$

The columns of **V** contain the orthonormal spatial basis functions, the orthonormal columns of **A** describe the time-dependence of the spatial basis functions, and **U** contains the weighting factors for the two matrixes **A** and **V**.

As a first step in processing the data, we apply this simplified PCA method to determine changes in oxyhemoglobin and deoxyhemoglobin, scaled by some pathlength factor *l* (see Kotz et al. 2006, included in appendix). The time-dependent images that describe $\Delta[Hb]$ and $\Delta[HbO_2]$ were ordered into a matrix as shown in equation (3), and the singular value decomposition was carried out to obtain the matrices **A**, **U**, and **V**. Figure 4 presents a plot of the normalized scaling factors contained along the diagonal of U. Only the first three or four eigenimages contribute significantly to the set of images that describe the hemoglobin dynamics in our study.

Figure 5 shows the first eigenimage corresponding to the first two columns of matrix **V**. The contrast between the tumor and the surrounding tissue is evident in the second image. The time-dependent weighting of the second eigenimage in the $\Delta[Hb](t)$ and $\Delta[HbO_2](t)$ sets of images can be determined from the matrix product of **A**•**U**, and is shown in Figure 6.

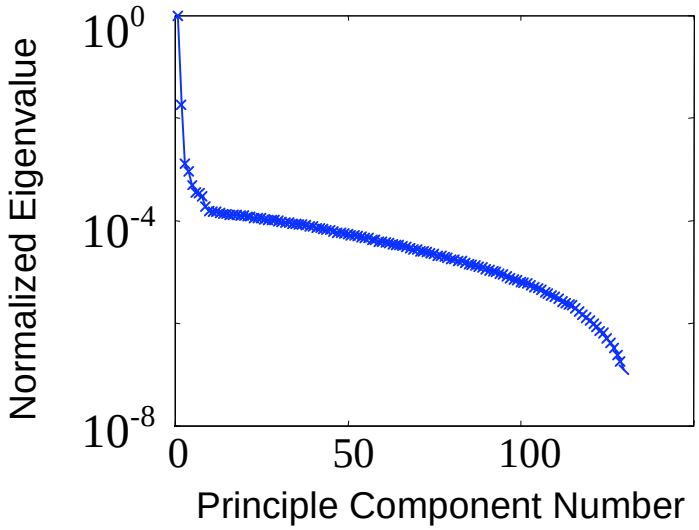

Figure 4. Normalized scaling factors (eigenvalues) for principal component analysis of image stack.

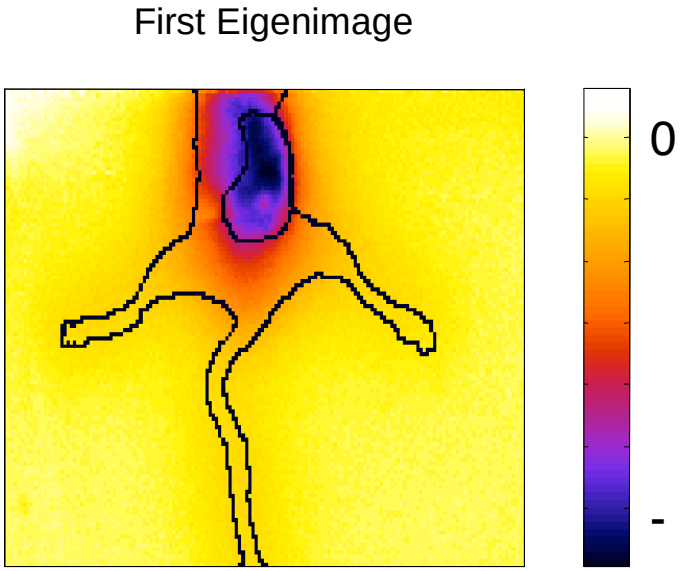

Figure 5. First eigenimage from principal component analysis.

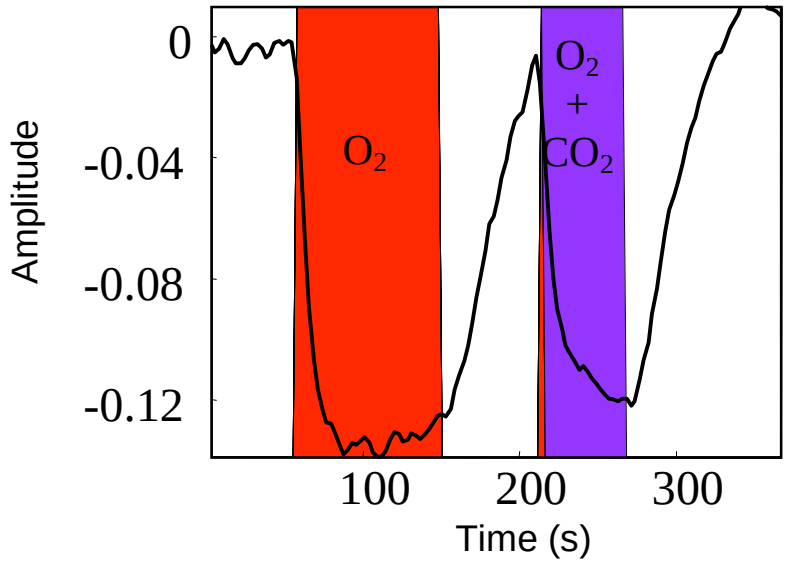

Figure 6. Time-dependent weighting of the first eigenimage from principal component analysis.

TASK 6. COMPARE DYNAMIC AND STATIC MEASUREMENTS

The response of the mouse to the gas inhalation protocols was assessed by examining the time-dependent sequence of images recorded at each wavelength. As a first step in the data analysis, we have recorded the mean and standard deviation of each background-subtracted image through time. The variation in pixel intensity through time gives a quantitative measure of the changes in the images in response to the inhaled gases. This variation in pixel intensity is shown in Figure 7 below for each of the wavelengths studied. The response is clearly enhanced in the regions of the tumor, and it appears as though the there is a enhancement in the response of the tumor to the gases. The general trends resulting from gas inhalation are consistent with point measurements observed by other researchers.[7]

The dynamics of the enhanced contrast between the tumor tissue and the mouse tissue due to the inhalation of the different gases was monitored by spatially averaging the changes in the image intensity over areas corresponding to signals due to cancerous tissue and areas due to normal tissues within the mouse. These averaged data are shown in Figure 8 for differences in the 780 nm and 840 nm images, respectively. The dashed line represents changes in the tumor

tissue, the thick solid line is for an adjacent region within the mouse that does not contain the tumor, and the line represents the average of a part of the image not containing the mouse. It is clear from both figures that there are distinct differences between the dynamics of the tumor tissue when compared with the normal mouse tissue. It is also clear that the response of the tissues is correlated to the presence of CO_2 in the 840 nm images, whereas the modulation of O_2 dominates the response at 780 nm.

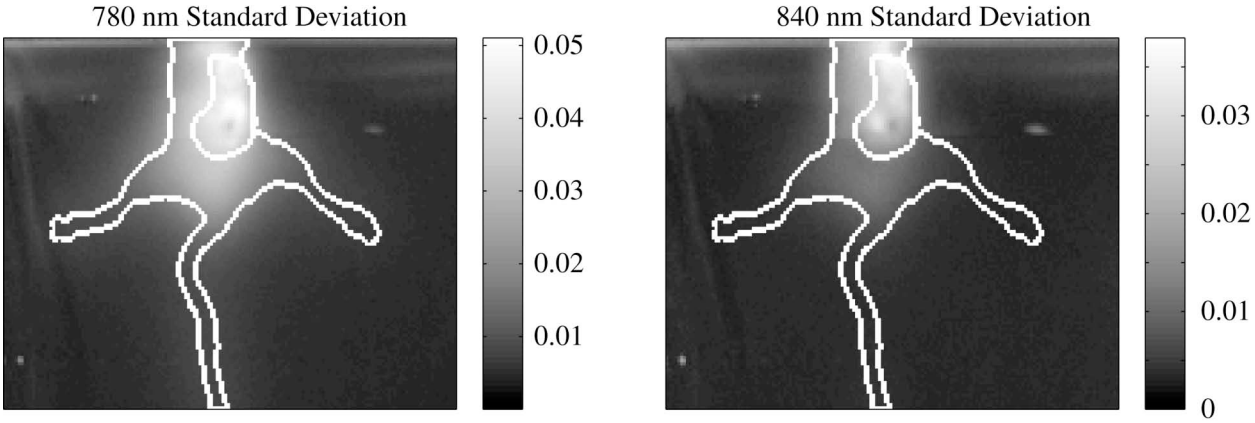

Figure 7. Standard deviations of the time-varying pixel absorbance values.

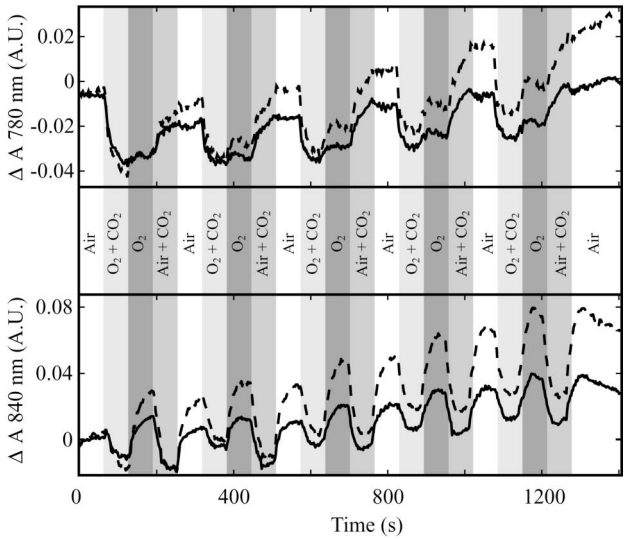

Figure 8. Dynamic response of the averaged signal due to the tumor tissue (dashed line) and the mouse tissue (solid line) at 780 nm and 840 nm.

We have also measured the static properties of the mouse tissue with the modified frequency domain apparatus. For these measurements, an anesthetized mouse was suspended between a U-shaped bar of aluminum. The mouse was held in place with a custom harness. The properties of the immersion media were measured as previously discussed, and following these measurements, the mouse was scanned between the source and detector fibers while measuring the amplitude and phase of the scattered signal. A sample scan recorded at 780 nm is shown below in Figure 9. Although the immersion media was not an exact match to the properties of the mouse, we were able to determine the average optical properties of the mouse tissues, and we were able to observe a region of the scan with anomalous scattering, which was correlated with the position of the tumor. We have used these results to further refine the exact scattering and absorption properties of the immersion media used in subsequent measurements.

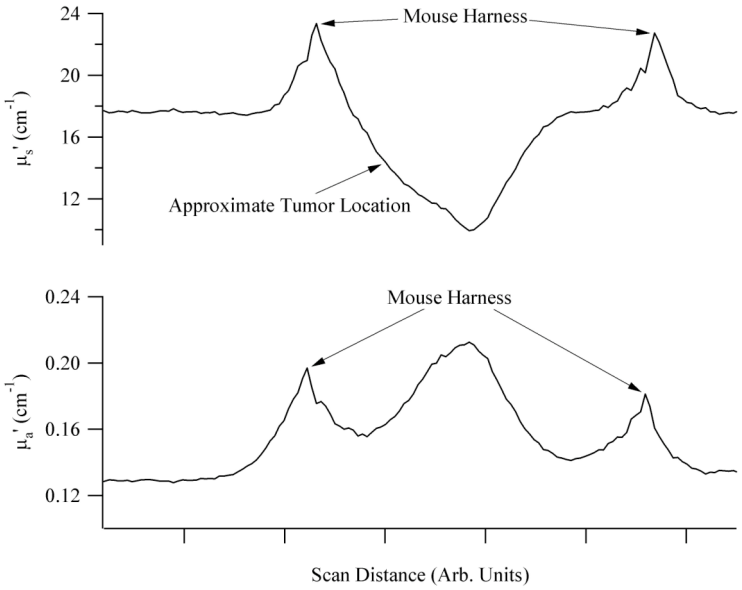

Figure 9. Scan of mouse tissue optical properties at 780 nm taken with frequency domain apparatus.

PERSONNEL

The following personnel were supported by this research effort:

Name	Role	Duties
Gregory Faris	Principal Investigator	Project Leadership
Kenneth Kotz	Postdoctoral Fellow	Experimental Studies
Konstantinos Kalogerakis	Investigator	Experimental Studies
Khalid Amin	Investigator	Animal Models
Juan Orduna	Investigator	Animal Models
Zhaohui Wang	Investigator	Animal Models
Wan-Ru Chao	Investigator	Animal Models
Barbara Sato	Investigator	Animal Models
Harold Javitz	Investigator	Statistician
David Watters	Investigator	Instrumentation Consulting
Steven Young	Technician	Electronics Support
Karl van Dyk	Technician	Mechanical Support
William Olson	Technician	Mechanical Support
Ross Jackson	Technician	Mechanical Support
Gabe Hernandez	Administrative Assistant	Technical Document Research

STUDENTS

The following students contributed to this research effort under support of the Research Experiences for Undergraduates Program of the National Science Foundation (NSF Physics).

Kendra Rand, a junior at Carthage College, Kenosha, WI

William Boenig, a junior at Santa Clara University, Santa Clara, CA

Nevena Rakuljic, a sophomore at University of California San Diego

Ashley Gibbs, a sophomore at Whitworth College

KEY RESEARCH ACCOMPLISHMENTS

We have achieved the following accomplishments on this project:

- Developed a simple and practical cw animal imaging system.
- Developed computer-controlled gas control system for easily variable animal inhalation experiments with on-demand gas mixing.
- Tested our approach on 5 animal tumor models.
- Compared static and dynamic contrasts mechanisms.
- Developed principal component analysis tools for image stack analysis.
- Shown dramatic contrast enhancement for our dynamic imaging method that is the basis for clinical studies.

REPORTABLE OUTCOMES

PUBLICATIONS

- K. S. Kalogerakis, K. T. Kotz, K. Rand, and G.W. Faris, "Animal imaging using immersion," Proc. SPIE **4955** (2003) 145-53. (See attached appendix)

- K. T. Kotz, K. S. Kalogerakis, W. N. Boenig, K. Amin, and G. W. Faris, "Dynamic imaging of tumor vasculature in rodents: Carbogen-induced contrast enhancement," Proc. SPIE 5312, 273-277 (2004). (See attached appendix)

- K. T. Kotz, K. Amin, J. M. Orduna, Z. A. Haroon, G. W. Faris, "Inspiratory Contrast for In Vivo Optical Imaging," submitted to Optics Letters (2006). (See attached appendix)

PRESENTATIONS

- K. Rand and G. W. Faris, "Breast Cancer Detection using Optical Vascular Function Imaging," Paper II.1, presented at 2002 Undergraduate Research Symposium in Mathematics and Physical Sciences, Pew Midstates Consortium, Washington University in St. Louis, 1-3 November 2002.

- K. S. Kalogerakis, K. T. Kotz, K. Rand, and G.W. Faris," Animal imaging using immersion," Paper 4955-21, presented at Optical Tomography and Spectroscopy of Tissue V, Photonics West, San Jose, California, 25-31 January 2003.

- K. T. Kotz, K. S. Kalogerakis, W. N. Boenig, K. Amin, and G. W. Faris "Dynamic Imaging of Tumor Vasculature in Rodents: Carbogen-induced Contrast Enhancement"

Paper 5312F-14 , presented at Innovations in Breast Cancer Diagnosis and Minimally Invasive Therapy, Photonics West, San Jose, California, 24-29 January 2004.

- K. T. Kotz, K. Amin, J. M. Orduna, W. A. Boenig, and G. W. Faris, "Image contrast enhancement following carbogen inhalation," Paper #275 ThF, presented at the OSA Biomedical Optics Topical Meeting, in Miami Beach, Florida, 14-17 April, 2004.

- K. T. Kotz, K. Amin, J. Orduna, W. A. Boenig, and G. W. Faris, "Imaging the dynamic tissue response to inhaled carbogen", Paper 1369, at the Optical Techniques for Medical Diagnosis, CLEO/IQEC, San Francisco, California, 16-21 May, 2004.

- K. T. Kotz, K. Amin, J. M. Orduna, W. A. Boenig, and G. W. Faris, "Image contrast enhancement following carbogen inhalation," Presented at NCI Optics Network (NTROI) Retreat, Newport Beach, CA, 3-5 June 3-5 2004.

- Kenneth T. Kotz, Khalid Amin, Juan M. Orduna, and Gregory W. Faris, "Imaging the vascular response to inhaled vasoactive compounds," Paper FThK3, presented at Frontiers in Optics 2004, The 88th Optical Society of America Annual Meeting, Rochester, NY, October 10-14, 2004.Kenneth T. Kotz, Khalid Amin, Juan M. Orduna, and Gregory W. Faris, "Near infrared in vivo imaging of the dynamic tissue response to vasoactive compounds," (Invited) Paper ANYL 183, presented at the 228th ACS National Meeting, Philadelphia, PA, August 22-26, 2004.

- K. T. Kotz, N. Rakuljic and G. W. Faris,, "Differential optical measurements of the dynamic tissue response to inhaled vasoactive gases," Paper 5693-72, presented at Optical Tomography and Spectroscopy of Tissue VII, Photonics West, San Jose, California, 22-27 January 2005.

- Kenneth T. Kotz, Khalid Amin, Juan M. Orduna, William A. Boenig, Ashley D. Gibbs, Christopher Comstock, and Gregory W. Faris, "Differential Optical Mammography,"

Paper B-25, presented at From Research to Action: Seeking Solutions, the 2005 California Breast Cancer Research Symposium, Sacramento, CA, September 9-11, 2005.

- Kenneth T. Kotz, Khalid Amin, Juan Orduna, and Gregory W. Faris, "Dynamic optical imaging of tumors following inhaled contrast agents," Paper FMI3, presented at Frontiers in Optics 2005, The 89th Optical Society of America Annual Meeting, Tucson, AZ, October 16-20, 2005.

- S. Dixit, K. T. Kotz, K. Amin, T. Le, A. Gibbs, and G. W. Faris, "Differential optical imaging for cancer detection using inspiratory contrast," Paper WD2, Presented at Optical Society of America Biomedical Optics Topical Meetings, Fort Lauderdale, Florida, March 19-22, 2006.

PATENT APPLICATION

- Gregory W. Faris, Kenneth T. Kotz, Mark Dewhirst, Konstantinos Kalogerakis, and Khalid Amin, Optical vascular function imaging system and method for detection and diagnosis of cancerous tumors," Patent Application Number PCT/US2005/003090, filed 21 January, 2005, International Publication Number WO2005070470 published 4 August 2005. (See attached appendix)

EMPLOYMENT

Kenneth Kotz, a postdoctoral fellow on this project, received multiple job offers and took a postdoctoral position at the Massachusetts General Hospital.

NEW FUNDING

Based on the success of this project, we applied for and were awarded funding to determine whether this imaging method can translate to the clinic. The California Breast Cancer

Research Program awarded this study to SRI International and the University of California San Diego.

CONCLUSIONS

We have shown that our dynamic imaging method can provide strong cancer-specific contrast in animal tumor models. Based on this project, funding is now in place for clinical studies of this non-invasive imaging method. If functional optical imaging can enhance early detection of breast cancer by detecting tumors missed on x-ray mammography (false negative results), it could reduce the economic and human cost associated with later detection of disease. If this approach can improve the diagnosis of breast cancer (reduce the number of false positive diagnoses), it could reduce the worry and economic cost of unnecessary biopsies. By providing more specific functional image information, optical imaging can enhance the ability to detect and diagnose cancer, compared with what is achievable with the physical image information provided by x-rays. For example, because of the low cost of optical instrumentation, optical imaging might be used in combination with x-ray mammography, which should provide greater sensitivity and specificity than x-rays alone. With the transition to digital x-ray mammography, optical imaging and x-ray mammography can even share the same camera, thereby providing excellent registration of the two modalities.

REFERENCES

1. M. Gerken and G. W. Faris, “High-accuracy optical-property measurements using a frequency domain technique,” Proc. SPIE **3597**, 593-600 (1999).
2. M. Gerken and G. W. Faris, “High-precision frequency-domain measurements of the optical properties of turbid media,” Opt. Lett. **24**, 930-932 (1999).
3. X. Wu and G. W. Faris, “Compensated transillumination,” Appl. Opt. **38**, 4262-4265 (1999).
4. S. Prahl, "Optical absorption of hemoglobin," from http://omlc.ogi.edu/spectra/hemoglobin/index.html (Oregon Medical Laser Center, 2003).
5. L. Sirovich and R. Everson, “Management and analysis of large scientific datasets,” Intl. J. Supercomputer Applications **6**, 50-68 (1992).
6. L. Sirovich and E. Kaplan, “Analysis methods for optical imaging,” in *Methods for In Vivo Optical Imaging of the Central Nervous System*, R. Frostig, Ed. (CRC Press, 2001).
7. J. G. Kim, D. Zhao, Y. Song, A. Constantinescu, R. P. Mason, and H. Liu, “Interplay of tumor vascular oxygenation and tumor pO_2 observed using near-infrared spectroscopy, an oxygen needle electrode, and ^{19}F MR pO_2 mapping,” J. Biomed. Opt. **8**, 53-62 (2003).

APPENDICES

- K. S. Kalogerakis, K. T. Kotz, K. Rand, and G.W. Faris, "Animal imaging using immersion," Proc. SPIE **4955** (2003) 145-53.

- K. T. Kotz, K. S. Kalogerakis, W. N. Boenig, K. Amin, and G. W. Faris, "Dynamic imaging of tumor vasculature in rodents: Carbogen-induced contrast enhancement," Proc. SPIE **5312**, 273-277 (2004).

- K. T. Kotz, K. Amin, J. M. Orduna, Z. A. Haroon, G. W. Faris, "Inspiratory Contrast for In Vivo Optical Imaging," submitted to Optics Letters (2006).

- Gregory W. Faris, Kenneth T. Kotz, Mark Dewhirst, Konstantinos Kalogerakis, and Khalid Amin, Optical vascular function imaging system and method for detection and diagnosis of cancerous tumors," Patent Application Number PCT/US2005/003090, filed 21 January, 2005, International Publication Number WO2005070470 published 4 August 2005.

Animal Imaging Using Immersion

Konstantinos S. Kalogerakis, Kenneth T. Kotz, Kendra Rand, and Gregory W. Faris[1]

Molecular Physics Laboratory, SRI International

333 Ravenswood Avenue

Menlo Park, CA 94025

ABSTRACT

We are using rodent animal models to study and compare contrast mechanisms for detection of breast cancer. These measurements are performed with the animals immersed in a matching scattering medium. The matching scattering medium or liquid tissue phantom comprises a mixture of Ropaque (hollow acrylic/styrene microspheres) and ink. We have previously applied matched imaging to imaging in humans. Surrounding the imaged region with a matched tissue phantom compensates for variations in tissue thickness and geometry, provides more uniform illumination, and allows better use of the dynamic range of the imaging system. If the match is good, the boundaries of the imaged region should almost vanish, enhancing the contrast from internal structure as compared to contrast from the boundaries and surface topography. For our measurements in animals, the immersion plays two additional roles. First, we can readily study tumors through tissue thickness similar to that of a human breast. Although the heterogeneity of the breast is lost, this is a practical method to study the detection of small tumors and monitor changes as they grow. Second, the immersion enhances our ability to quantify the contrast mechanisms for peripheral tumors on the animal because the boundary effects on photon migration are eliminated. We are currently developing two systems for these measurements. One is a continuous-wave (CW) system based on near-infrared LED illumination and a CCD (charge-coupled device) camera. The second system, a frequency domain system, can help quantify the changes observed with the CW system.

Keywords: Compensated transillumination, frequency-domain measurements, animal models, breast cancer, tumor detection, *in vivo* imaging.

1. INTRODUCTION

The observation of illumination through tissue, known as transillumination or diaphanography, was one of the first methods employed for medical imaging, dating back to the early 19th century.[1,2] Optical mammography was first performed in 1929.[3] The introduction of cooler light sources and the use of film or a camera to detect near-infrared wavelengths generated considerable research activity in breast transillumination during the 1970's and 1980's.[4-6] Nevertheless, optical mammography proved inferior to x-ray mammography.[7,8] The primary problem with optical mammography is poor spatial resolution, which reduces contrast in smaller tumors. However, this limitation can be reduced or even overcome by providing functional (physiological) imaging information.

There has been a resurgence of interest in optical techniques for breast cancer detection in the past decade, spurred on by better understanding of light propagation through tissue,[9,10] time-resolved optical techniques for imaging,[11-15] better quantification of tissue properties,[16,17] and new image reconstruction algorithms.[18-20] This interest has been reflected in

[1] Corresponding author (Email: gregory.faris@sri.com, Tel.: 650-859-4131, Fax: 650-859-6196).

Optical Tomography and Spectroscopy of Tissue V, Britton Chance, Robert R. Alfano, Bruce J. Tromberg, Mamoru Tamura, Eva Marie Sevick-Muraca, Editors, Proceedings of SPIE Vol. 4955 (2003)

the development of industrial prototype imaging systems at Philips,[12] Zeiss,[14] and Siemens.[15] Applications of advanced optical mammography techniques have shown promising results.[14,21-24] Several research groups are examining the use of contrast agents for breast cancer detection.[24-28] Others have performed animal studies using window chambers to provide direct optical access to study the microenvironment of a tumor.[29,30] A number of *ex vivo* studies of the optical properties of normal and diseased breast tissue have also been performed.[31-33]

One limitation for *in vivo* optical imaging is due to non-uniform thickness and variable geometry. Small variations in the thickness of the illuminated tissue lead to large variations in the intensity of transmitted light. Asymmetries in the location and orientation of the tissue surface cause variations in the reflectivity of the tissue. Additionally, light may be lost or diffuse away at tissue boundaries transverse to the imaging plane. In combination, these effects cause significant variations in the intensity of the transmitted light and reduce contrast within the observed tissue. In some cases, the undesired effects of intensity variation can be reduced by measuring the optical path length and by making the corresponding adjustments to the image contrast. This approach has been applied in frequency-domain techniques where the phase shift of an amplitude-modulated light beam was used to determine the optical path length.[34] In our experiments, the uniformity and contrast of the image is improved by immersing the imaged tissue in a liquid medium with the same absorption and scattering behavior as the tissue under study. Such matching of the optical properties by immersion results in a more uniform image and in optimized contrast. When a good match is achieved, the tissue boundaries will practically disappear, and the contrast in the image will mainly reflect variations in internal structure. In addition, imaging in a matching liquid medium usually results in improved and more uniform illumination conditions.

Matching techniques have been used in the past for the determination of tissue properties[16,35,36] and for scanned time-resolved optical mammography.[37,38] Previous work at SRI International has combined CW imaging with immersion in a matching medium to obtain images of the human hand.[39] A conventional incandescent lamp illuminated a Plexiglas box containing the matching medium, a mixture of Ropaque, water and methylene blue dye. Matching between the human tissue and relative concentration of the dye and Ropaque was achieved with frequency-domain measurements.[36,40] Images of a human hand immersed in the matching medium were recorded with an intensified CCD and a conventional camera. Comparisons with images recorded without immersion showed that images with immersion display more detail and internal structure than can be seen without the matching conditions.[39]

While x-ray imaging primarily reveals structural information, optical imaging provides both structural information and information on tissue function through the use of optical spectroscopy. Spectroscopic information may be enhanced through application of time-resolved methods such as time-domain or frequency-domain techniques to provide quantitative information on chemical state or composition. For example, optical measurements performed at different wavelengths can provide information on total hemoglobin content and hemoglobin oxygenation.[42] This type of functional information is significant for breast cancer detection. The angiogenesis associated with tumor growth typically leads to elevated local hemoglobin concentrations.[22,23,43] In addition, tumors exhibit atypical vasculature and vasoactivity, and are often hypoxic, a condition that can be observed optically by hemoglobin oxygenation measurements. Tumor hypoxia may also be used to guide treatment because more hypoxic tumors are likely to be metastatic or invasive.[44-46] The distinct morphology of tumors has also been shown to provide a source of contrast through variations in the optical scattering coefficient.[47]

In this proceeding, we present results from preliminary experiments inspired by a new form of functional optical imaging. The main objective is to study the contrast enhancement available using inspiration of varying amounts of carbon dioxide and oxygen. These studies are being performed in rodents. The animal model employed allows the study of contrast during tumor progression and over a range of tumor sizes. We use imaging by immersion in a matching medium to improve quantification, simplify measurements on the small animals, and simulate tissue depth similar to that of the human breast. These studies attempt to use the full range of available optical contrast by augmenting functional optical imaging using dynamic measurements related to tumor vascular function associated with inspired gases. The broadest use of available contrast will be most effective for improving sensitivity and specificity in tumor detection and monitoring.

2. EXPERIMENTAL APPARATUS AND RESULTS

We are using two optical systems for our studies—a frequency domain system for quantification and a CW system for monitoring rapid changes. Both systems use immersion of the animals in liquid tissue phantoms to improve the uniformity and contrast of the images and facilitate quantification for the small volumes imaged.

The first instrument is based on the frequency domain approach, a rather simple and accurate method for quantitative optical measurements of tissue properties. This technique uses measurements of the optical delay of light through a medium to quantitatively determine absorption and scattering properties on human or animal tissue. The phase shift of the modulated light increases with the amount of scatter, while its amplitude decreases with absorption by the medium. A simplified schematic diagram of a frequency domain measurement system developed in our laboratory is shown in Figure 1. An oscillator modulates a light source at a radio frequency (RF) of 100 MHz. This light is carried to the measured region through an optical fiber. A second fiber carries scattered light to a detector. A mixer detects the amplitude and RF phase of the modulated light. By measuring the changes in the DC and RF amplitudes and the RF phase of the detected signal as a function of source-detector separation, we can determine the absorption and scattering coefficients of the measured tissue region.[48] This frequency-domain system has a precision of better than 1% for measurements on homogeneous tissue phantoms.[40]

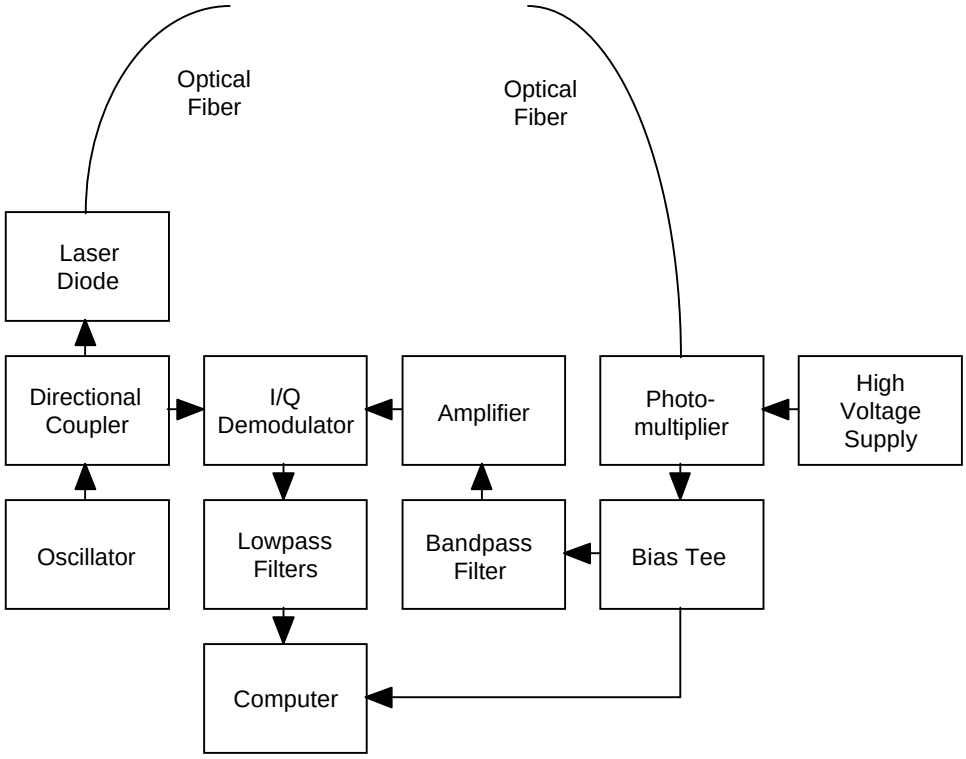

Figure 1. Schematic diagram of the frequency-domain imaging system.

Once the absorption and scattering behavior of the immersion medium has been characterized, the only measurements required to measure a tissue sample are the differences in phase and amplitude with and without the sample between the optical fiber bundles. Thus, the determination of the absorption coefficient, μ_a, and the reduced scattering coefficient, μ_s', as a function of wavelength, time, or position, is a straightforward matter.

We use the CW instrument to examine the dynamic physiological behavior. These measurements are performed using a CW source and a two-dimensional detector, such as a CCD or conventional camera. The instrumentation for this immersion-based imaging, or compensated transillumination, is shown in Figure 2. The system comprises an LED (light-emitting diode) array as the illumination source, filters, a box for the immersion medium, and a CCD camera. Two types of LED arrays are currently used with output radiation centered at 780 and 840 nm, respectively. The imaging system is suitable for a fast frame acquisition rate and averaging. Switching between LED arrays enables measurements at different wavelengths and the determination of hemoglobin content and hemoglobin oxygenation.[42]

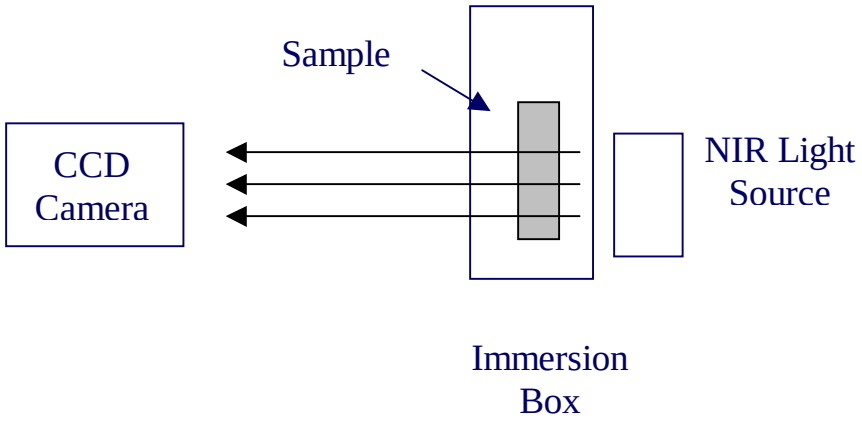

Figure 2. Schematic diagram of the CW immersion imaging system.

The studies of vascular function imaging are performed on animal breast cancer models (rats with chemically induced tumors and nude mice with tumor xenografts). We use animal models because they allow monitoring contrast on a range of tumor sizes and stages of development. Furthermore, the measurements are noninvasive and thus can be readily repeated on animals as our instrumentation and methods are refined. Measurement through tissue thickness similar to the human breast can be performed by partially immersing the anesthetized animals in liquid tissue phantoms that simulate the optical properties of breast tissue. Although this approach does not include the effects of tissue heterogeneity in the breast, it is the most practical method for studying contrast over a range of tumor sizes.

In this paper, we present preliminary results from our imaging studies. Figure 3 shows an image of a nude mouse recorded with our CW imaging apparatus operating at 780 nm. The anesthetized mouse is attached by its legs onto a 3mm Plexiglass platform with black tape. The Plexiglass platform is placed in the immersionbox in a manner such that the mouse is illuminated from the front and its abdomen is facing the light source. The immersion box is filled with a tissue phantom approximating the absorption and scattering properties of the mouse. The tumor, which has a diameter of approximately 1 cm, can be distinguished clearly as the bright circle on the lower part of the left side of the image. The head of the mouse is outside of the immersion box, above the surface of the tissue phantom and is not included in the image. Part of the tail of the mouse can be seen at the bottom of the image. The mouse has been anesthetized by injection of sodium pentobarbital and is breathing ambient air. The image presented is a single still frame and no averaging has been performed.

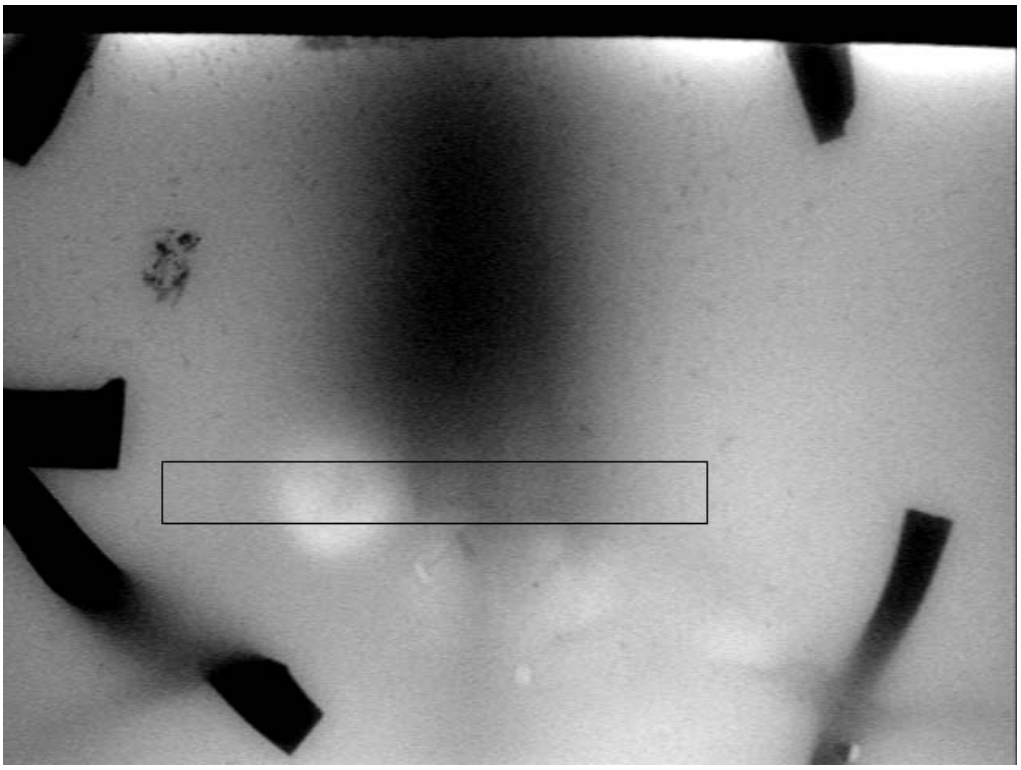

Figure 3. Image of a nude mouse with tumor obtained by compensated transillumination at 780 nm.

Figure 4 presents an intensity profile obtained by integrating the light intensity in the rectangular area shown in Fig. 3. The central part of the mouse's body is the darker region and the tumor the brighter one. A slope exists in the baseline illumination intensity between the left and right part of the image. Future experiments will address this issue and include improvements in the instrumentation so as to achieve better illumination uniformity and image symmetry. Nevertheless, even from a single frame, it is possible to identify readily the location and size of the tumor as well as the relative hemoglobin concentration.

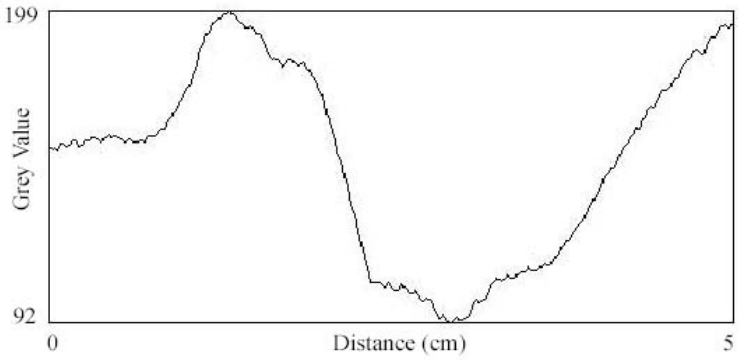

Figure 4. Caption for profile graph with cross section through tumor

The appearance of the tumor in Fig. 3 as a bright spot indicates lack of blood content relative to the surrounding tissue. This result is most likely a manifestation of tumor necrosis and indicates that the imaging is capable of distinguishing between different types of tumors, e.g., a tumor deprived of blood vs. one filled with blood. Our apparatus allows the study of the progression of the tumor and monitoring of any necrotic tissue as it expands. In future experiments, we plan to investigate these possibilities by studying different types of tumors, by performing an autopsy on the animal after the experiments, by using more than one wavelength for the illumination, and by administering carbogen gas to the animal under study.

4. DISCUSSION

The vasculature produced through angiogenesis in tumors has atypical characteristics, which in turn provide the basis for our imaging approach. Blood vessels in tumors are often highly abnormal, exhibiting distended capillaries with leaky walls and sluggish flow. These properties of tumor vasculature provide at least three different types of contrast for optical imaging in conjunction with varying levels of inspired oxygen and carbon dioxide. These types of contrast are due to low oxygenation improvement, atypical vasoactivity, and blood pooling. First, when elevated levels of oxygen are administered, the oxygenation rise in tumors is typically much lower than that of normal tissue types.[50-52] Second, tumor vasculature often shows vasoactivity in opposition to that of normal tissues, for example exhibiting vasodilation while normal tissue vasoconstricts.[53,54] It has been shown that tumor vasculature vasoconstricts in response to carbogen (95% O_2/5% CO_2) administration,[55,56] which is the opposite of what would be anticipated. Further evidence of compromised microvascular control has also been observed through measurements of NADH signals by Dr. Britton Chance and collaborators.[57] As both oxygen and carbon dioxide are vasoactive, atypical tumor behavior from administration of changing levels of these gases should provide strong imaging contrast. Finally, as tumor vessels are often contorted and leaky, any blood pooling in these vessels will lead to delayed response to oxygenation changes, providing another good contrast mechanism.

Additional facts motivate investigations of dynamic contrast associated with tumor vascular function. First, the breast is highly heterogeneous, comprising the lobes (glandular tissue), fat, connective tissue, ducts, and the supporting vasculature. We believe that using a broader palette of contrast mechanisms will provide more specificity for optical imaging and help compensate for the heterogeneity of the breast. Second, the more successful noninvasive optical measurements, such as pulse oximetry and functional brain imaging, are dynamic in nature. In pulse oximetry,[58,59] the dynamic signal of the cardiac pulse is combined with the optical signals of oxygenated and deoxygenated hemoglobin to derive blood oxygenation levels without detailed knowledge of the tissue type and level of scattering. For brain imaging,[60-63] dynamic measurements of hemoglobin or hemoglobin oxygenation are performed during specific mental tasks such as finger tapping or visual stimulus. The successes of these approaches, which combine dynamic and functional information, lead us to apply a similar combination of dynamic and functional measurements for the studies proposed here. Finally, recent theoretical work has demonstrated improved results from differential optical imaging.[64,65] Dynamic and differential imaging techniques are similar in that they both rely on changes in optical contrast over time.

By providing more specific functional image information, we believe that optical imaging can enhance the ability to detect and diagnose cancer, compared to what is achievable with the physical image information provided by x-rays. In addition, because of the low cost of the optical instrumentation we are using, optical imaging could be used easily in combination with x-ray mammography, and their synergy should provide greater sensitivity and specificity than x-rays alone.

ACKNOWLEDGMENTS

This work is supported by the U.S. Army Breast Cancer Research Program. The participation of Kendra Rand was funded by the Research Experiences for Undergraduates Program of the National Science Foundation (NSF Physics). We are grateful to Khalid Amin, Juan Orduña, and Zhaohui Wang for helpful discussions and assistance with animal handling and to Dr. Mark Dewhirst for helpful discussions.

REFERENCES

1. T. B. Curling, "Simple Hydrocele of the Testis," in *A Practical Treatise on the Diseases of the Testis and of the Spermatic Cord and Scrotum*, pp. 125-181, Samuel Highley, London, 1843.
2. R. Bright, "Diseases of the Brain and Nervous System," in *Reports of Medical Cases Selected with a View of Illustrating the Symptoms and Cure of Diseases by a Reference to Morbid Anatomy,* Vol. II, Case CCV, p. 431, Longman, Rees, Orms, Brown and Green, London, 1831.
3. M. Cutler, "Transillumination as an aid in the diagnosis of breast lesions," Surg. Gynecol. Obstet. **48,** pp. 721-729, 1929.
4. C. Gros, Y. Quenneville, and Y. Hummel, "Diaphanologie mammaire [Breast diaphanology]," J. Radiol. Electrol. Med. Nucl. **53,** pp. 297-306, 1972.
5. B. Ohlsson, J. Gundersen, and D.-M. Nilsson, "Diaphanography: A method for evaluation of the female breast," World J. Surg. **4,** pp. 701-707, 1980.
6. C. H. Jones and S. P. Newbery, "Visualization of superficial vasculature using a vidicon camera tube with silicon target," Br. J. Radiol. **50,** pp. 209-210, 1977.
7. R. F. Girolamo and J. V. Gaythorpe, "Clinical diaphanography — Its present perspective," CRC Crit. Rev. Oncol./Hematol. **2,** pp. 1-31, 1989.
8. A. Alveryd, I. Andersson, K. Aspegren, G. Balldin, N. Bjurstam *et al*., "Lightscanning versus mammography for the detection of breast cancer in screening and clinical practice. A Swedish multicenter study," Cancer **65,** pp. 1671-1677, 1990.
9. M. S. Patterson, B. Chance, and B. C. Wilson, "Time resolved reflectance and transmittance for the non-invasive measurement of tissue optical properties," Appl. Opt. **28,** pp. 2331-2336, 1989.
10. R. C. Haskell, L. O. Svaasand, T.-T. Tsay, T.-C. Feng, M. S. McAdams, and B. J. Tromberg, "Boundary conditions for the diffusion equation in radiative transfer," J. Opt. Soc. Am. A **11,** pp. 2727-2741, 1994.
11. T. O. McBride, B. W. Pogue, E. D. Gerety, S. B. Poplack, U. L. Österberg, and K. D. Paulsen, "Spectroscopic diffuse optical tomography for the quantitative assessment of hemoglobin concentration and oxygen saturation in breast tissue," Appl. Opt. **38,** pp. 5480-5490, 1999.
12. S. B. Colak, D. G. Papaioannou, G. W. 't Hooft, M. B. van der Mark, H. Schomberg, J. C. J. Paasschens, J. B. M. Melissen, and N. A. A. J. van Asten, "Tomographic image reconstruction from optical projections in light-diffusing media," Appl. Opt. **36,** pp. 180-213, 1997.
13. M. A. O'Leary, D. A. Boas, B. Chance, and A. G. Yohd, "Experimental images of heterogeneous turbid media by frequency-domain diffusing-photon tomography," Opt. Lett. **20,** pp. 426-428, 1995.
14. K. T. Moesta, S. Fantini, H. Jess, S. Totkas, M.-A. Franceschini, M. Kaschke, and P. M. Schlag, "Contrast features of breast cancer in frequency-domain laser scanning mammography," J. Biomed. Opt. **3,** pp. 129-136, 1998.
15. H. Heusmann, J. Kölzer, and G. Mitic, "Characterization of female breasts in vivo by time resolved and spectroscopic measurements in near infrared spectroscopy," J. Biomed. Opt. **1,** pp. 425-434, 1996.
16. M. Gerken and G. W. Faris, "Frequency-domain immersion technique for accurate optical property measurements of turbid media," Opt. Lett. **24,** pp. 1726-1728, 1999.
17. S. Fantini, M. A. Franceschini, J. B. Fishkin, B. Barbieri, and E. Gratton, "Quantitative determination of the absorption spectra of chromophores in strongly scattering media: A light-emitting-diode based technique," Appl. Opt. **33,** pp. 5204-5213, 1994.
18. H. Jiang, K. D. Paulsen, U. L. Osterberg, B. W. Poque, and M. S. Patterson, "Optical image reconstruction using frequency-domain data: Simulations and experiments," J. Opt. Soc. Am. A **13,** pp. 253-266, 1996.
19. S. R. Arridge and M. Schweiger, "A gradient-based optimisation scheme for optical tomography," Opt. Express **2,** pp. 213-226, 1998.
20. M. J. Eppstein, D. E. Dougherty, T. L. Troy, and E. M. Sevick-Muraca, "Biomedical optical tomography using dynamic parameterization and Bayesian conditioning on photon migration measurements," Appl. Opt. **38,** pp. 2138-2150, 1999.
21. Q. Zhu, E. Conant, and B. Chance, "Optical imaging as an adjunct to ultrasound in differentiating benign from malignant lesions," Proc. SPIE **3597,** pp. 532-539, 1999.

22. J. B. Fishkin, O. Coquoz, E. R. Anderson, M. Brenner, and B. J. Tromberg, "Frequency-domain photon migration measurements of normal and malignant tissue optical properties in a human subject," Appl. Opt. **36,** pp. 10-20, 1997.
23. B. Chance, E. Anday, E. Conant, S. Nioka, S. Zhou, and H. Long, "Rapid and sensitive optical imaging of tissue functional activity, and breast," in *Advances in Optical Imaging and Photon Migration*, edited by James G. Fujimoto and Michael S. Patterson, pp. 218-225, Optical Society of America, Washington, DC, 1998.
24. J. S. Reynolds, T. L. Troy, R. H. Mayer, A. B. Thompson, D. J. Waters, K. K. Cornell, P. W. Snyder, and E. M. Sevick Muraca, "Imaging of spontaneous canine mammary tumors using fluorescent contrast agents," Photochem. Photobiol. **70,** pp. 87-94, 1999.
25. D. J. Bornhop, D. S. Hubbard, M. P. Houlne, C. Adair, G. E. Kiefer, B. C. Pence, and D. L. Morgan, "Fluorescent tissue site-selective lanthanide chelate, Tb-PCTMB for enhanced imaging of cancer," Anal. Chem. **71,** pp. 2607-2615, 1999.
26. D. A. Benaron, "Imaging cancer in vivo using optical markers in animal and human subjects, Paper 4259B-25," presented at the Molecular Probes and Dyes, Photonics West, San Jose, CA, 2001.
27. G. W. Faris and M. J. Dyer, "Upconverting chelates for biomedical diagnostics," presented at the Biomedical Topical Meetings, Miami Beach, FL, April 2000.
28. B. Riefke, K. Licha, and W. Semmler, "Contrast media for optical mammography," Radiologe **37,** pp. 749-755, 1997.
29. R. Melder, H. Salehi, and R. Jain, "Interaction of activated natural killer cells with normal and tumor vessels in cranial windows in mice," Microvasc. Res. **50,** pp. 35-44, 1995.
30. M. W. Dewhirst, E. T. Ong, R. D. Braun, B. Smith, B. Klitzman, S. M. Evans, and D. Wilson, "Quantification of longitudinal tissue pO_2 gradients in window chamber tumours: Impact on tumour hypoxia," Br. J. Cancer **79,** pp. 1717-1722, 1999.
31. T. L. Troy, D. L. Page, and E. M. Sevick-Muraca, "Optical properties of normal and diseased breast tissues," in *Biomedical Optical Spectroscopy and Diagnostics*, edited by E. Sevick-Muraca and D. Benaron, pp. 59-66, Optical Society of America, Washington, DC, 1996.
32. H. Key, E. R. Davies, P. C. Jackson, and P. N. T. Wells, "Optical attenuation characteristics of breast tissues at visible and near-infrared wavelengths," Phys. Med. Biol. **36,** pp. 579-590, 1991.
33. V. G. Peters, D. R. Wyman, M. S. Patterson, and G. L. Frank, "Optical properties of normal and diseased human breast tissues in the visible and near infrared," Phys. Med. Biol. **35,** pp. 1317-1334, 1990.
34. S. Fantini, M. A. Franceschini, G. Gaida, E. Gratton, H. Jess, W. W. Mantulin, K. T. Moesta, P. M. Schlag, and M. Kaschke, "Frequency-Domain Optical Mammography: Edge Effect Corrections," Med. Phys. **23,** pp. 149-157, 1996.
35. H. Liu, M. Miwa, B. Beauvoit, N. G. Wang, and B. Chance, "Characterization of absorption and scattering properties of small-volume biological samples using time-resolved spectroscopy," Anal. Biochem. **213,** pp. 378-385, 1993.
36. X. Wu, L. Stinger, and G. W. Faris, "Determination of tissue properties by immersion in a matched scattering fluid," Proc. SPIE **2979,** pp. 300-306, 1997.
37. S. Zhou, C. Xie, S. Nioka, H. Liu, Y. Zhang, and B. Chance, "Phased-array instrumentation appropriate to high-precision detection and localization of breast tumor," Proc. SPIE **2979,** pp. 98-106, 1997.
38. X. D. Li, J. P. Culver, T. Durduran, B. Chance, A. G. Yodh, and D. N. Pattanayak, "Diffraction Tomography with Diffuse Photon Density Waves: Clinical Studies and Background Subtraction," in *Advances in Optical Imaging and Photon Migration*, edited by James G. Fujimoto and Michael S. Patterson, pp. 281-283, Optical Society of America, Washington, DC, 1998.
39. X. Wu and G. W. Faris, "Compensated transillumination," Appl. Opt. **38,** pp. 4262-4265, 1999.
40. M. Gerken and G. W. Faris, "High-precision frequency-domain measurements of the optical properties of turbid media," Opt. Lett. **24,** pp. 930-932, 1999.
41. J. T. Bruulsema, J. E. Hayward, T. J. Farrell, M. S. Patterson, L. Heinemann *et al.*, "Correlation between blood glucose concentration in diabetics and noninvasively measured tissue optical scattering coefficient," Opt. Lett. **22,** pp. 190-192, 1997.
42. S. Wray, M. Cope, D. T. Delpy, J. S. Wyatt, and E. O. R. Reynolds, "Characterization of the near infrared absorption spectra of cytochrome aa_3 and haemoglobin for the non-invasive monitoring of cerebral oxygenation," Biochim. Biophys. Acta **933,** pp. 184-192, 1988.

43. B. J. Tromberg, N. Shah, R. Lanning, A. Cerussi, J. Espinoza, T. Pham, L. Svaasand, and J. Butler, "Non-invasive in vivo characterization of breast tumors using photon migration spectroscopy," Neoplasia **2,** pp. 26-40, 2000.
44. P. Okunieff, M. Hoeckel, E. P. Dunphy, K. Schlenger, C. Knoop, and P. Vaupel, "Oxygen tension distributions are sufficient to explain the local response of human breast tumors treated with radiation alone," Int. J. Radiat. Oncol. Biol. Phys. **26,** pp. 631-636, 1993.
45. D. M. Brizel, G. S. Sibley, L. R. Prosnitz, R. L. Scher, and M. W. Dewhirst, "Tumor hypoxia adversely affects the prognosis of carcinoma of the head and neck," Int. J. Radiat. Oncol. Biol. Phys. **38,** pp. 285-289, 1997.
46. P. Vaupel, O. Thews, D. K. Kelleher, and M. Hoeckel, "Oxygenation of human tumors: The Mainz experience," Strahlenther Onkol. **174,** pp. 6-12, 1998.
47. M. Holboke, B. Tromberg, X. Li, N. Shah, J. Fishkin, D. Kidney, J. Butler, B. Chance, and A. Yodh, "Three-dimensional diffuse optical mammography with ultrasound localization in a human subject," J. Biomed. Opt. **5,** pp. 237-247, 2000.
48. M. Gerken and G. W. Faris, "High-accuracy optical-property measurements using a frequency domain technique," Proc. SPIE **3597,** pp. 593-600, 1999.
49. B. Chance, M. Cope, E. Gratton, N. Ramanujam, and B. Tromberg, "Phase measurement of light absorption and scatter in human tissue," Rev. Sci. Instrum. **69,** pp. 3457-3481, 1998.
50. D. M. Brizel, S. Lin, J. L. Johnson, J. Brooks, M. W. Dewhirst, and C. A. Piantadosi, "The mechanisms by which hyperbaric oxygen and carbogen improve tumour oxygenation," Br. J. Cancer **72,** pp. 1120-1124, 1995.
51. J. L. Lanzen, R. D. Braun, A. L. Ong, and M. W. Dewhirst, "Variability in blood flow and pO_2 in tumors in response to carbogen breathing," Int. J. Radiat. Oncol. Biol. Phys. **42,** pp. 855-859, 1998.
52. G. Stuben, M. Stuschke, K. Knuhmann, M. R. Horsman, and H. Sack, "The effect of combined nicotinamide and carbogen treatments in human tumour xenografts: Oxygenation and tumour control studies," Radiother. Oncol. **48,** pp. 143-148, 1998.
53. G. D. Kennovin, F. W. Flitney, and D. G. Hirst, ""Upstream" modification of vasoconstrictor responses in rat epigastric artery supplying an implanted tumour," Adv. Exp. Med. Biol. **345,** pp. 411-416, 1994.
54. K. M. Bell, D. J. Chaplin, B. A. Poole, V. E. Prise, and G. M. Tozer, "Modification of blood flow in the HSN tumour and normal tissues of the rat by the endothelin ET(B) receptor agonist, IRL 1620," Int. J. Cancer **80,** pp. 295-302, 1999.
55. M. W. Dewhirst, E. T. Ong, G. L. Rosner, S. W. Rehmus, S. Shan, R. D. Braun, D. M. Brizel, and T. W. Secomb, "Arteriolar oxygenation in tumour and subcutaneous arterioles: Effects of inspired air oxygen content," Br. J. Cancer Suppl. **27,** pp. S241-S246, 1996.
56. B. M. Fenton, E. M. Lord, and S. F. Paoni, "Enhancement of tumor perfusion and oxygenation by carbogen and nicotinamide during single- and multifraction irradiation," Radiat. Res. **153,** pp. 75-83, 2000.
57. B. Chance, personal communication, 2000.
58. J. W. Severinghaus and J. F. Kelleher, "Recent developments in pulse oximetry," Anesthesiology **76,** pp. 1018-1038, 1992.
59. J. Sinex, "Pulse oximetry: Principles and limitations," Am. J. Emerg. Med. **17,** pp. 59-67, 1999.
60. M. A. Franceschini, V. Toronov, M. E. Filiaci, E. Gratton, and S. Fantini, "On-line optical imaging of the human brain with 160-ms temporal resolution," Opt. Express **6,** pp. 49-57, 2000.
61. B. Chance, E. Anday, S. Nioka, S. Zhou, L. Hong *et al.*, "A novel method for fast imaging of brain function, non-invasively, with light," Opt. Express **2,** pp. 411-423, 1998.
62. D. A. Benaron, S. R. Hintz, A. Villringer, D. Boas, A. Kleinschmidt *et al.*, "Noninvasive functional imaging of human brain using light," J. Cereb. Blood Flow Metab. **20,** pp. 469-477, 2000.
63. M. Tamura, Y. Hoshi, and F. Okada, "Localized near-infrared spectroscopy and functional optical imaging of brain activity," Phil. Trans. R. Soc. Lond. B Biol. Sci. **352,** pp. 737-742, 1997.
64. V. Ntziachristos, B. Chance, and A. Yodh, "Differential diffuse optical tomography," Opt. Express **5,** pp. 230-242, 1999.
65. R. L. Barbour, S. Zhong, H. L. Graber, Y. Pei, S.-L. S. Barbour *et al.*, "Optical tomographic cinematography of vascular reactivity," presented at the Optical Society of America Annual Meeting, Santa Clara, CA, 1999.

Dynamic Imaging of Tumor Vasculature in Rodents: Carbogen-induced Contrast Enhancement

Kenneth T. Kotz, Konstantinos S. Kalogerakis, William N. Boenig,
Khalid Amin, and Gregory W. Faris*
Molecular Physics Laboratory, SRI International
333 Ravenswood Avenue
Menlo Park, CA 94025

ABSTRACT

We have studied the dynamic changes in tissue vasculature following the inhalation of hyperoxic gasses in rodents as a model for optical breast cancer detection. We have used a CW apparatus to measure the near infrared (NIR) optical properties of animal models immersed in a liquid tissue phantom. By looking at the transmission of different wavelengths in the NIR, we were able to qualitatively observe changes in blood oxygenation following the inhalation of different mixtures of CO_2 and O_2. These changes enhanced the image contrast between cancerous tissue and normal tissues of the rodents. The oxygenation dynamics of the tumors, following inhalation of the hyperoxic gases, exhibited differences from surrounding tissues in both the magnitude of the observed signal change and the dynamic response.
Keywords: Compensated transillumination, animal models, tumor vasculature, breast cancer, tumor detection, *in vivo* imaging contrast enhancement.

1. INTRODUCTION

The near infrared (NIR) region between 700 nm and 900 nm provides a relatively transparent spectral window for observing physiologically important chemical compounds. Two of the important NIR absorbers in tissue are oxygenated (HbO_2) and deoxygenated hemoglobin (Hb) and thus this region of the spectrum is ideal for measuring tissue oxygenation.[1] It is well established that tumors exhibit abnormalities in vasculature such as abrupt endings of vessels, abnormal branching, and increased leakiness (permeability).[2] Many tumors are also often hypoxic which is a powerful stimulus for the angiogenesis (development of new blood vessels) leading to growth and invasiveness of the tumor. Many researchers have attempted to improve the oxygenation of cancerous tissues through the inhalation of increased levels of oxygen, which makes them more vulnerable to certain treatments such as radiation.[3] Tissue oxygenation can be measured with a number of standard techniques, however, results are typically referenced to an oxygen electrode invasively embedded within the tumor.[4] Recently, Liu et al. have attempted to monitor such efforts toward oxygenation improvement through the *in vivo* NIR absorption and pO_2 electrode measurements of cancerous tumors in rat models.[5]

Tumors are known to have distinct vasoactivity in the presence of vasoactive compounds. Recent studies have shown that increased levels of inspired O_2 leads to vasoconstriction of all blood vessels, while increased levels of inspired CO_2 leads to constriction of mature arteries only, leaving the intratumoral neovasculature unaltered.[6] We believe that these properties may lead to a mechanism for optical contrast in static diffuse NIR transmission images. *In vivo* optical imaging of hemodynamics in the NIR has the potential to give not only structural information, but also information regarding tissue function, as inferred through the quantitative information on the chemical composition of tissues determined by optical spectroscopy. Thus, we have recorded

* Corresponding author (Email: gregory.faris@sri.com, Tel.: 650-859-4131, Fax: 650-859-6196).

Lasers in Surgery XIV, Bartels, Bass, de Riese, Gregory, Hirschberg, Katzir, Kollias, Madsen, Malek, McNally-Heintzelman, Paulsen, Robinson, Tate, Trowers, Wong, Eds., Proc. of SPIE Vol. 5312
(SPIE, Bellingham, WA, 2004) · 1605-7422/04/$15 · doi: 10.1117/12.538888

dynamic measurements of the blood oxygenation parameters of mice in response to varying levels of inspiratory hypercapnia (elevated CO_2) and hyperoxia (elevated O_2) not only as a guide to treatment but also as a novel imaging modality for cancer detection.

2. EXPERIMENTAL

2.1 Animal model

In this study, female athymic nude mice (20-25g, Harlan Laboratories) were injected with mouse embryonic fibrosarcoma (MEF), U87 (Brain Tumor) or human breast cancer (MDA 231) cells administered subcutaneously on the dorsum of the mice. All of these cell lines were used at a concentration of 2-3 million cells in 100 µl of medium for each animal. The tumor volumes were measured twice weekly once they attain a measurable size. In principle, these xenograft models allow the study of contrast during tumor progression and over a range of tumor sizes. Animals were anesthetized with pentobarbital (30-40mg/kg) injected intraperitoneally at the beginning of the experiment.

2.2 Imaging apparatus

The instrument used to measure the optical properties of these mice is shown below in Fig. 1. The anesthetized animals were partially immersed in a temperature controlled (37-38° C) medium that matched the optical properties of the mice (Ropaque and water).[7] Infrared light from the LEDs (780 nm and 840 nm) was passed through the immersion box and collected with a digital monochrome CCD camera (Point Grey Research) through a 16 mm f/0.95 lens (JML Optics). Mass flow controllers (MDC) regulate the levels of oxygen and carbon dioxide with respect to ambient air delivered to the mice through a custom nose cone at constant rate of 4.2 L/min. Other experiments have shown no effects from rebreathing at this flow rate.[6] The camera, LEDs, gas concentrations, and temperature measurement are interfaced to and controlled by a laptop computer. Image data is stored and post-processed using MATLAB and ImageJ.

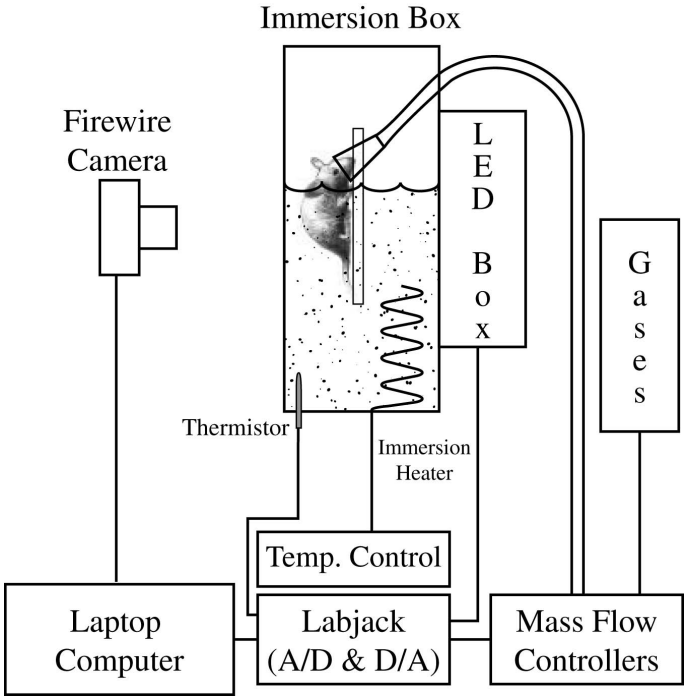

Fig. 1. Experimental Apparatus

3. RESULTS

We used this apparatus to image the CW NIR optical transmission properties of the animals. The transmission through the mice and the immersion medium were measured at the different wavelengths mentioned above (780 nm and 840 nm), while the gas concentrations were changed. We cycled between ambient air, carbogen (95% O_2 and 5% CO_2), 100% O_2, and 95% air/5% CO_2. Differential absorption images were calculated by a procedure similar to that found in the literature.[1,3] Briefly, we subtracting the logarithm of a baseline (pre-protocol) image from the logarithm the images at each time point. Then, by using the extinction coefficients of Hb and HbO_2, we converted the differential wavelength images into qualitative changes in the concentrations of oxygenated and deoxygenated hemoglobin (Δ[Hb] and Δ[HbO_2], respectively). For these experiments, we did not correct for the scattering in the absorption measurements, and thus the numeric values given in the figures are qualitative. In order to quickly assess the overall changes that occur during the experimental run, we take the average and standard deviation of the pixels through time corresponding to the Δ[Hb] and Δ[HbO_2] images. These are shown below in Fig 2.

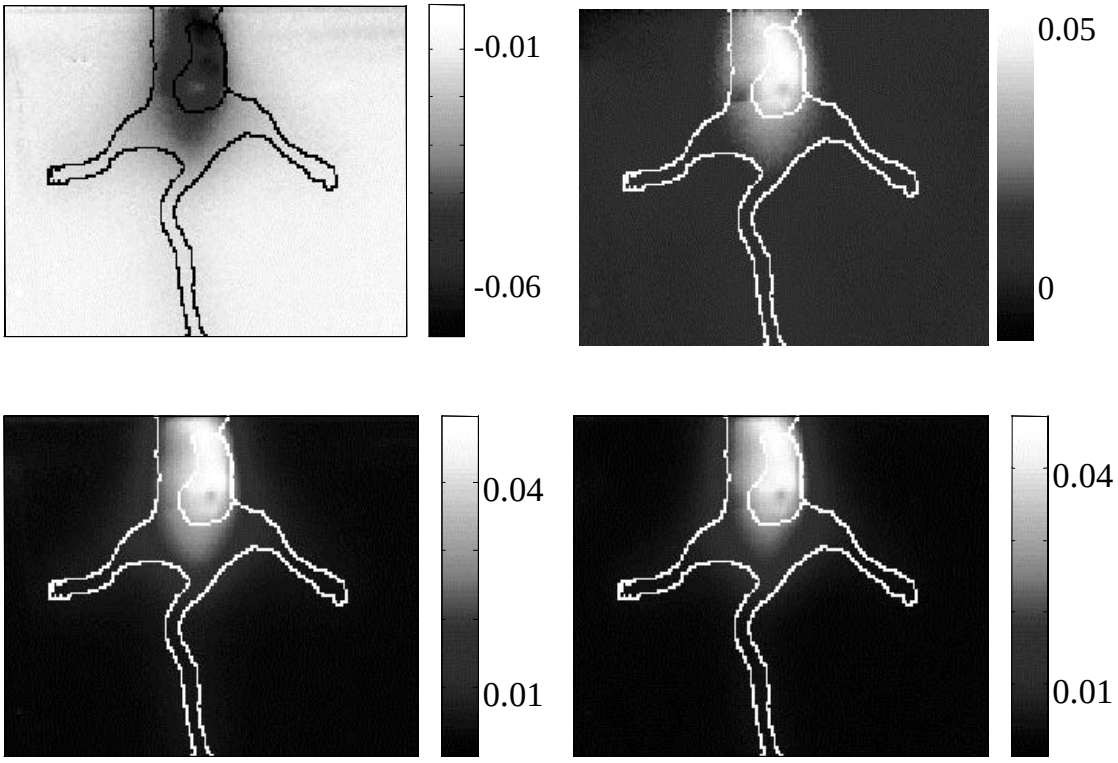

Fig.2. Response of calculated Δ[Hb] and Δ[HbO_2] to gas inhalation. The left hand images correspond to Δ[Hb] and the right to Δ[HbO_2]. The top images are the time averaged mean values and the bottom images represent the standard deviations from the mean. The approximate outline of the mouse and the tumor is overlaid on the images as a guide to the reader. These were determined after the experiment by draining the tank and taking an image that was registered to the dynamic measurements.

The images above show distinct regions of high contrast in the tumor region. By looking through time at the average values of the pixels above a threshold in the standard deviation images, we can get an idea of the dynamics of the tissue vasculature for either the mouse body or the region of the tumor (Fig. 3). It can be seen in Fig. 3 that the tumor region exhibits a larger response to the mouse tissue and that both responses are highly

correlated with the delivery of oxygen to the animal (r~0.8). The signal in both cases is characterized by a very fast response (<10 s) to the introduction of the O_2 followed by a very slow decay back to the baseline (~30-45 s). These results are consistent with similar single-point measurements found in the literature.[3,8] Furthermore, the dynamics of the tumor region do not decay back to the baseline, but seem to dip below it. These are all general trends seen in all the mice that we have studied thus far.

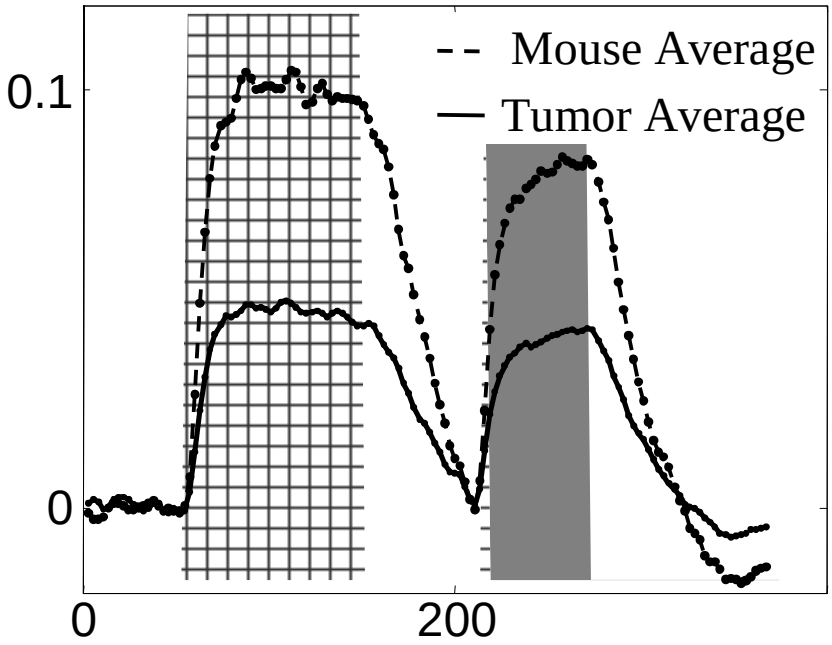

Fig.3. ΔHbO_2 dynamics in two different regions of the images. The dashed line represents the average of the pixels that span the region of the lower right-hand image of Fig. 1 above a threshold of 0.04, corresponding to changes in the tumor tissue. The solid line represents the average of the pixels that span the region of the lower right-hand image of Fig. 1 between the values of 0.009 and 0.04, corresponding to changes in the mouse tissue. The bar with light gray cross-hatches corresponds to 100% O_2 delivery to the mouse, the dark gray bar corresponds to 95% O_2 + 5% CO_2 gas delivery to the mouse.

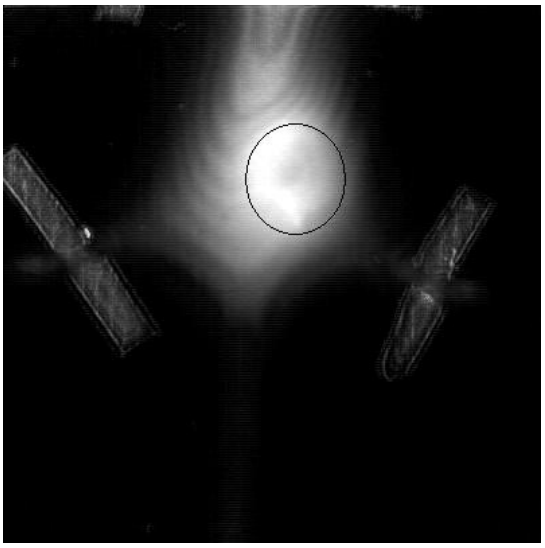

Fig.4. Response of mouse vasculature to gas inhalation as seen in the standard deviation of HbO_2 difference images. The oval in the image represents the approximate location of the cancerous tumor.

Fig. 4 shows another image of the standard deviations of pixels for the $\Delta[HbO_2]$ values for a different mouse with a MEF tumor. Again, the inhalation of O_2 leads to the enhancement of the image contrast in the region of the tumor. We are currently working on the quantifying the changes in the $\Delta[HbO_2]$ and $\Delta[Hb]$ images, and on extracting the dynamics from tumor irrespective of the surrounding mouse tissue. The current results, however, suggest that the inhalation of gases can act as a significant contrast mechanism in functional optical imaging. This project was funded by the DOD Breast Cancer Research Program, DAMD170920109570. We acknowledge helpful conversations with Dr. Mark Dewhirst and Dr. Zishan Haroon of Duke University Medical Center.

References:

1. Tuchin, V. V. (ed.) *Handbook of Optical Biomedical Diagnostics* (SPIE Press, Bellingham, WA, 2002).
2. Vaupel, P., Kallinowski, F. & Okunieff, P. "Blood Flow, Oxygen and Nutrient Supply, and Metabolic Microenvironment of Human Tumors", *Cancer Research*, **49**, 6449-6465, 1989.
3. Gu, Y. et al. "Dynamic response of breast tumor oxygenation to hyperoxic respiratory challenge monitored with three oxygen-sensitive parameters", *Applied Optics*, **42**, 2960-2967, 2003.
4. Horsman, M. R. "Measurement of Tumor Oxygenation", *Int. J. Radiation Oncology Biol. Phys.*, **42**, 701-704, 1998.
5. Kim, J. G. et al. "Interplay of tumor vascular oxygenation and tumor pO2 observed using near-infrared spectroscopy, an oxygen needle electrode, and 19F MR pO2 mapping", *Journal of Biomedical Optics*, **8**, 53-62, 2003.
6. Neeman, M., Dafni, H., Bukhari, O., Braun, R. D. & Dewhirst, M. W. "In vivo BOLD contrast MRI mapping of subcutaneous vascular function and maturation: validation by intravital microscopy", *Magn. Reson. Med.*, **45**, 887-898, 2001.
7. Wu, X. & Faris, G. W. "Compensated transillumination", *Applied Optics*, **38**, 4262-4265, 1999.
8. Hull, E. L., Conover, D. L. & Foster, T. H. "Carbogen-induced changes in rat mammary tumour oxygenation reported by near infrared spectroscopy", *Br. J. Cancer*, **79**, 1709-1716, 1999.

Inspiratory Contrast for *In Vivo* Optical Imaging

Kenneth T. Kotz, Khalid Amin, Juan M. Orduna, Zishan A. Haroon, Gregory W. Faris

SRI International, 333 Ravenswood Ave. Menlo Park, CA 94025

We show that inhalation of oxygen and carbon dioxide leads to significant contrast for *in vivo* optical imaging. Differential imaging in a rodent cancer model provides up to a factor of two variation in signal change between tumor and normal tissue. This exogenous enhancement of the endogenous contrast due to oxy- and deoxyhemoglobin appears quite promising for cancer detection.

OCIS codes: (170.0110) Imaging Systems; (170.6510) Spectroscopy, tissue diagnostics; (170.5280) Photon migration

Differential or dynamic optical imaging[1,2] provides a number of advantages including a reduced sensitivity to boundary effects and improved sensitivity. These advantages are borne out in two examples of successful optical measurements in vivo. Functional optical imaging of the brain[3,4] is only feasible through the use of differential imaging. Pulse oximetry,[5,6] perhaps the most successful clinical use of light in human tissue, is also based on differential measurements.

During the process of angiogenesis, tumors develop abnormal vasculature, and as a result, cancerous tissue is often hypoxic, a condition that can be observed with hemoglobin oxygenation measurements. Hypoxic tumors are also likely to be metastatic or invasive, and as a

consequence, measurements to monitor blood oxygenation parameters have been carried out in order to guide the treatment of such tumors.[7-9] We believe that it should be possible to use the endogenous contrast afforded by spectroscopic properties of hemoglobin with the addition of exogenous vasoactive agents as a method to improve detection of cancerous tumors with optical techniques.

For this study, the differential imaging of vasoactivity is performed through the transillumination measurements on a tumor model in nude mice. For the tumor model, female athymic nude mice (20-25g, Harlan Laboratories) were injected with mouse embryonic fibrosarcoma (MEF), U87 (brain tumor), A549 (lung tumor) or human breast cancer (MDA 231) cells administered subcutaneously on the dorsum of the mice. All of these cell lines were used at a concentration of 2-3 million cells in 100 µl of medium for each animal. The tumor volumes were measured twice weekly once they attain a measurable size. Animals were anesthetized with pentobarbital (30-40 mg/kg) injected intraperitoneally at the beginning of the experiment. A schematic of the instrument used to measure the transillumination of these mice is shown in Fig. 1. The anesthetized animals were partially immersed in a temperature controlled (37-38° C) medium that matched the optical properties of the mice (Ropaque and water, μ_a = .08 cm^{-1}, μ_s = 12 cm^{-1}).[10] Infrared light from the LEDs (780 nm and 840 nm, Epitex, Inc.) passed through the immersion box and collected with a digital monochrome CCD camera (Dragonfly, Point Grey Research) through a 16 mm f/0.95 lens (JML Optics). Mass flow controllers (MDC) regulate the levels of air, oxygen, and carbon dioxide, which are delivered to the mice via a custom nose cone at a constant total flow rate of 4.2 L/min. The camera, LEDs, gas concentrations, and temperature measurement are interfaced to and controlled by a laptop computer on a mobile platform. Image data is stored and post-processed using MATLAB and ImageJ.

Using this apparatus, CW transillumination measurements were recorded at each wavelength. Differential absorption images were obtained by subtracting the logarithm of a baseline image (pre-protocol) from the logarithm of the remaining images taken at later times while the gas concentrations were changed between ambient, hyperoxic (carbogen (95% O_2 and 5% CO_2) or 100% O_2) and hypercapnic (95% air and 5% CO_2) conditions. Using the extinction coefficients of Hb and HbO_2,[11] and Beer's Law, we converted the differential wavelength images into changes in the concentrations of oxygenated and deoxygenated hemoglobin (Δ[Hb] and $\Delta[HbO_2]$, respectively).[12] For these experiments, we did not correct for the scattering in the absorption measurements, and thus the numeric values given in the figures are qualitative.

In order to visualize the changes in the images, we take the mean and standard deviation of each pixel through time. The standard deviation image for [Δ HbO_2], shown in Fig. 2, indicates the magnitude of the changes in concentration of oxygenated hemoglobin for the image sequences, and demonstrates the remarkable enhancement in differential contrast between cancerous and non-cancerous tissues in response to vasoactive gases. As expected, the majority of the response is contained within the tumor boundaries. The dynamic response of the tumorigenic and non-tumorigenic tissues can be estimated by spatially averaging over the pixels outlining the tumor and the mouse body, respectively, for each image throughout the measurement sequence (Fig. 3). The measured dynamics exhibit similar trends to those measured with point-source apparatus,[7,8] namely, that the concentration of oxy-hemoglobin increases with hyperoxia while the concentration of deoxy-hemoglobin decreases, and that the total concentration of hemoglobin remains approximately constant. Previous researchers have also observed heterogeneity of the oxygenation improvement within individual tumors by inserting oxygen-measuring probes into the tumor mass at different sites.[13] Spatial

heterogeneities can be seen in Fig. 2, suggesting that our non-invasive optical imaging technique is capable of probing such changes.

Using this apparatus, we have examined many different tumor models. Each of the models exhibits the same trends that are shown in Fig. 2 and Fig. 3. By further increasing the fraction of CO_2 delivered to the mouse to 15%, we have been able to see changes in the signals at 780 nm and 840 nm, which seem well correlated with the presence of O_2 or CO_2, respectively, as shown in Fig. 4. It is commonly believed that vasoconstriction results from breathing pure O_2, whereas a small fraction of CO_2 has a vasodilatory effect on the mature blood vessels. Recent work combining microscopy and MRI have suggested, however, that both hypercapnia and hyperoxia lead to vessel constriction; hypercapnia leads to constriction of mature arteries, whereas hyperoxia leads constriction of all vessels.[14] We believe that the signal changes in Fig. 4 are due to the direct vasoresponse to the specific hyperoxic or hypercapnic inhalatory conditions. Currently, it is difficult to quantitatively assess the values for the total concentration of hemoglobin, and thus it is difficult to directly compare our results with others. Improvements in the imaging apparatus in Fig. 1 are currently underway, and should provide us with the

We find that inhalation of varying levels of oxygen and carbon dioxide provides strong cancer-specific contrast in animals. This approach may prove useful for small animal imaging of cancer models or for cancer imaging in humans.

This research was supported by funds from DOD Breast Cancer Research Program, Grant Number DAMD17-02-1-0570 and the California Breast Cancer Research Program of the University of California, Grant Number 10EB-0168. We acknowledge helpful conversations with Dr. Mark Dewhirst of Duke University Medical Center.

Figure Captions

Fig. 1. Schematic of the experimental apparatus.

Fig. 2. (Color online) Standard deviations of the individual pixel values for $\Delta[HbO_2]$ time-series of images.

Fig. 3. Plot of $\Delta[Hb]$ (**a**) and $\Delta[HbO_2]$ (**b**) for U87 brain tumor (dashed line) and normal tissue (solid) in response to gas inhalation. Gas concentrations were 100% Air, 100 O_2 or 95% O_2 + 5% CO_2, as labeled in the figure.

Fig. 4. Change in absorption at 780 nm (**a**) and 840 nm (**b**) for A549 lung tumor (dashed line) and normal tissue (solid) in response to gas inhalation. Gas concentrations were 100% Air, 100 O_2 or 95% O_2 + 5% CO_2, as labeled in the figure.

References

1. V. Ntziachristos, B. Chance, and A. Yodh, Opt. Express **5**, 230 (1999).

2. R. L. Barbour, H. L. Graber, Y. Pei, S. Zhong, and C. H. Schmitz, J. Opt. Soc. Am. A **18**, 3018 (2001).

3. M. A. Franceschini, V. Toronov, M. E. Filiaci, E. Gratton, and S. Fantini, Opt. Express **6**, 49 (2000).

4. B. Chance, E. Anday, S. Nioka, S. Zhou, L. Hong, K. Worden, C. Li, T. Murray, Y. Ovetsky, D. Pidikiti, and R. Thomas, Opt. Express **2**, 411 (1998).

5. J. W. Severinghaus and J. F. Kelleher, Anesthesiology **76**, 1018 (1992).

6. J. Sinex, Am. J. Emerg. Med. **17**, 59 (1999).

7. Y. Gu, V. A. Bourke, J. G. Kim, A. Constantinescu, R. P. Mason, and H. Liu, Appl. Opt. **42**, 2960 (2003).

8. E. L. Hull, D. L. Conover, and T. H. Foster, Br. J. Cancer **79**, 1709 (1999).

9. H. W. Wang, M. E. Putt, M. J. Emanuele, D. B. Shin, E. Glatstein, A. G. Yodh, and T. M. Busch, Cancer Res. **64**, 7553 (2004).

10. X. Wu and G. W. Faris, Appl. Opt. **38**, 4262 (1999).

11. S. A. Prahl, "Tabulated Molar Extinction Coefficients for Hemoglobin in Water," from http://omlc.ogi.edu/spectra/hemoglobin/index.html (2004).

12. J. G. Kim, D. Zhao, Y. Song, A. Constantinescu, R. P. Mason, and H. Liu, J. Biomed. Opt. **8**, 53 (2003).

13. O. Thews, D. K. Kelleher, and P. Vaupel, Radiother. Oncol. **62**, 77 (2002).

14. M. Neeman, H. Dafni, O. Bukhari, R. D. Braun, and M. W. Dewhirst, Magn. Reson. Med. **45**, 887 (2001).

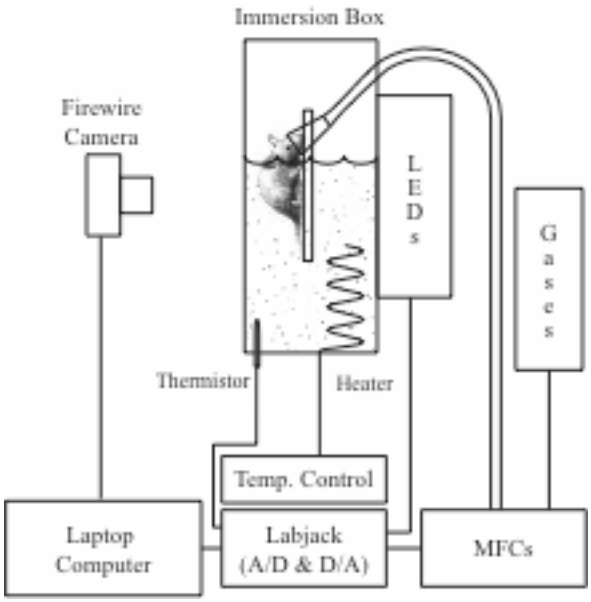
Immersion Box
Firewire
Camera
LEDs
Gases
Thermistor
Heater
Temp. Control
Laptop
Computer
Labjack
(A/D & D/A)
MFCs

Figure 1

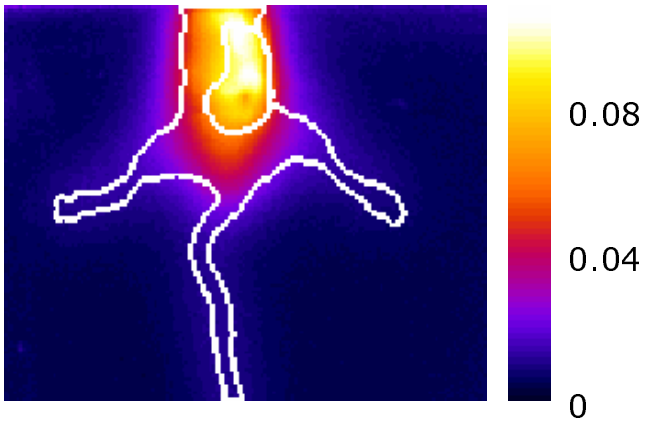

Figure 2

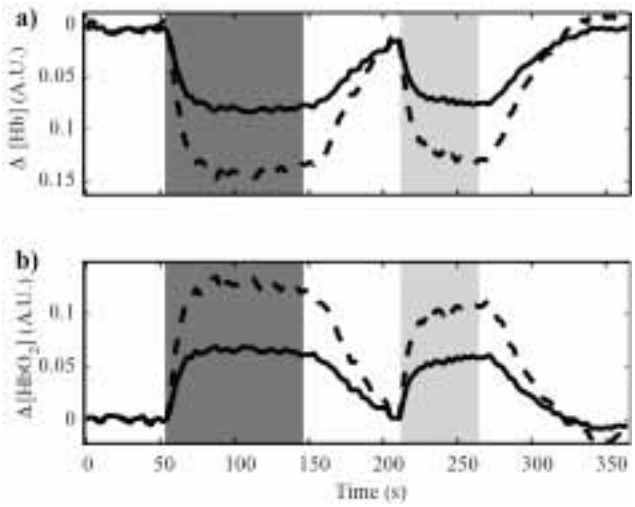
a)
0
0.05
0.1
0.15
Δ [Hb] (A.U.)
b)
0.1
0.05
0
Δ[HbO2] (A.U.)
0
50
100
150
200
250
300
350
Time (s)

Figure 3

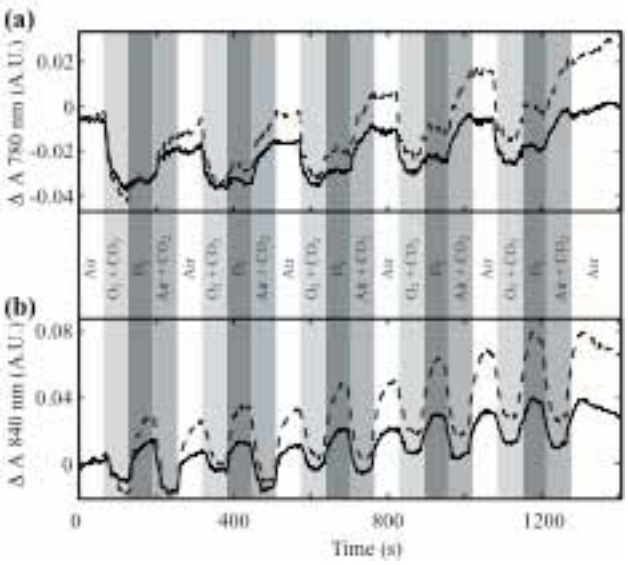
(a)
Δ A 780 nm (A.U.)
0.02
0
-0.02
-0.04
Air
O2 + CO2
Ar
Ar + CO2
Air
O2 + CO2
Ar
Ar + CO2
Air
O2 + CO2
Ar
Ar + CO2
Air
O2 + CO2
Ar
Ar + CO2
Air
(b)
Δ A 840 nm (A.U.)
0.08
0.04
0
0
400
800
1200
Time (s)

Figure 4

(12) INTERNATIONAL APPLICATION PUBLISHED UNDER THE PATENT COOPERATION TREATY (PCT)

(19) World Intellectual Property Organization
International Bureau

(43) International Publication Date
4 August 2005 (04.08.2005)

PCT

(10) International Publication Number
WO 2005/070470 A1

(51) International Patent Classification[7]: A61K 49/00

(21) International Application Number:
PCT/US2005/003090

(22) International Filing Date: 21 January 2005 (21.01.2005)

(25) Filing Language: English

(26) Publication Language: English

(30) Priority Data:
60/538,765 23 January 2004 (23.01.2004) US

(71) Applicant *(for all designated States except US)*: **SRI INTERNATIONAL** [US/US]; 333 Ravenswood Avenue, Menlo Park, CA 94025 (US).

(72) Inventor; and
(75) Inventor/Applicant *(for US only)*: **FARIS,Gregory, W.** [US/US]; 2042 santa Cruz Avenue, Menlo Park, CA 94025 (US).

(74) Agents: **ALBOSZTA, Marek** et al.; Lumen IPS, 2345 Yale Street, 2nd Floor, Palo Alto, CA 94306 (US).

(81) Designated States *(unless otherwise indicated, for every kind of national protection available)*: AE, AG, AL, AM, AT, AU, AZ, BA, BB, BG, BR, BW, BY, BZ, CA, CH, CN, CO, CR, CU, CZ, DE, DK, DM, DZ, EC, EE, EG, ES, FI, GB, GD, GE, GH, GM, HR, HU, ID, IL, IN, IS, JP, KE, KG, KP, KR, KZ, LC, LK, LR, LS, LT, LU, LV, MA, MD, MG, MK, MN, MW, MX, MZ, NA, NI, NO, NZ, OM, PG, PH, PL, PT, RO, RU, SC, SD, SE, SG, SK, SL, SY, TJ, TM, TN, TR, TT, TZ, UA, UG, US, UZ, VC, VN, YU, ZA, ZM, ZW.

(84) Designated States *(unless otherwise indicated, for every kind of regional protection available)*: ARIPO (BW, GH, GM, KE, LS, MW, MZ, NA, SD, SL, SZ, TZ, UG, ZM, ZW), Eurasian (AM, AZ, BY, KG, KZ, MD, RU, TJ, TM), European (AT, BE, BG, CH, CY, CZ, DE, DK, EE, ES, FI, FR, GB, GR, HU, IE, IS, IT, LT, LU, MC, NL, PL, PT, RO, SE, SI, SK, TR), OAPI (BF, BJ, CF, CG, CI, CM, GA, GN, GQ, GW, ML, MR, NE, SN, TD, TG).

Published:
— *with international search report*

For two-letter codes and other abbreviations, refer to the "Guidance Notes on Codes and Abbreviations" appearing at the beginning of each regular issue of the PCT Gazette.

WO 2005/070470 A1

(54) Title: OPTICAL VASCULAR FUNCTION IMAGING SYSTEM AND METHOD FOR DETECTION AND DIAGNOSIS OF CANCEROUS TUMORS

(57) Abstract: An *in vivo* optical imaging system and method of identifying unusual vasculature associated with the angiogenic vasculature in tumors. An imaging system acquires images through the breast. Benign, noninvasive oxygen and carbon dioxide are used as vasoactive agents and administered by inhalation to stimulate vascular changes. Images taken before and during inhalation are subtracted. An optical vascular functional imaging system monitors abnormal vasculature through optical measurements on oxy- and deoxyhemoglobin during inhalation of varying levels of O_2 and CO_2. The increase in contrast between tumor (cancerous) and normal (noncancerous) tissue is dramatic, facilitating accurate early detection of cancerous tumors and improving sensitivity and specificity (lower false negative and false positive rates). The invention is useful in mammography, dermatology, prostate imaging and other optically accessible areas.